Data to Knowledge: Understanding Dynamic Medical Images

Computer Science (CS) is the new language of science as Mathematics was until the Twentieth Century. CS generalizes mathematics toward being more versatile. In this talk we will focus on some problems in bio-medical science and discuss how our group views the challenges and how we try to address them computationally.

Tomography is the technology of combining data from multiple views (say, 2D camera snapshots) to create a comprehensive image (say, in 3D). In medicine tomography is used to gather knowledge about target organs or physiology inside patients without any probing surgery. In vivo molecular imaging, or gene expression analysis in real time, is a promised goal of functional imaging. However, it involves time-varying signals coming from inside the body. My talk is on some of the projects on nuclear imaging and fluorescent imaging data with different types of dynamics in order to elicit bio-medical information.

Debasis Mitra is a Professor in the Department of Computer Science at Florida Institute of Technology in Melbourne. His current interest is in Imaging and Data Sciences, specially in medical imaging and molecular biology. In the past he has worked on Artificial Intelligence and Mathematical Physics.

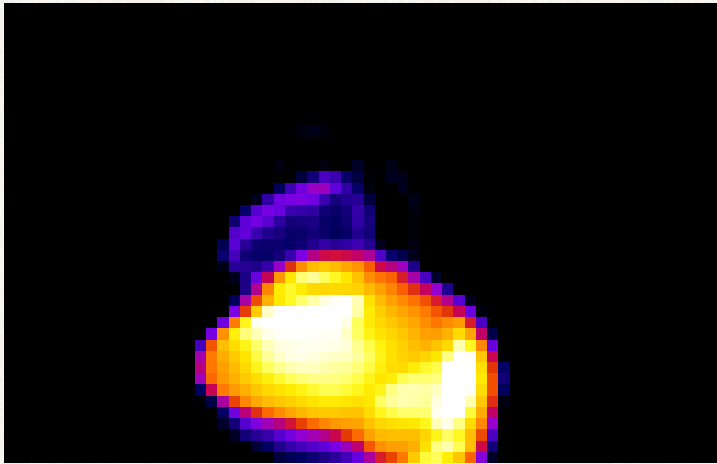# Data to Knowledge: Understanding Dynamic Medical Images

Debasis Mitra

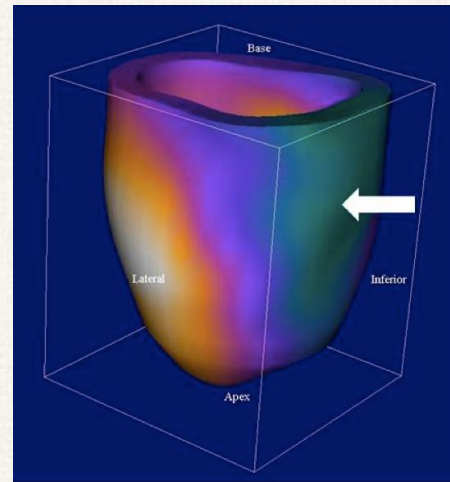**Department of Computer Sciences**
Florida Institute of Technology

Image credit: Mahmoud Abdalah and www

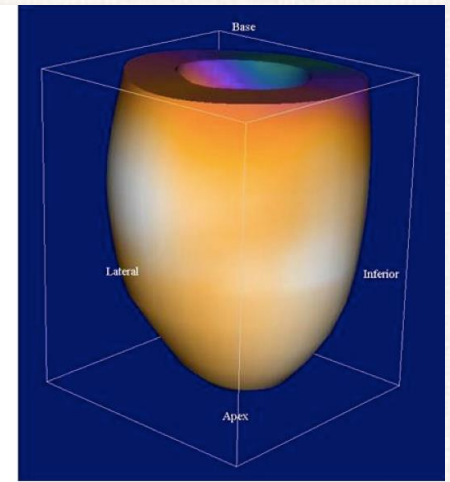# Tomography: Non-invasive Probing of Human Body

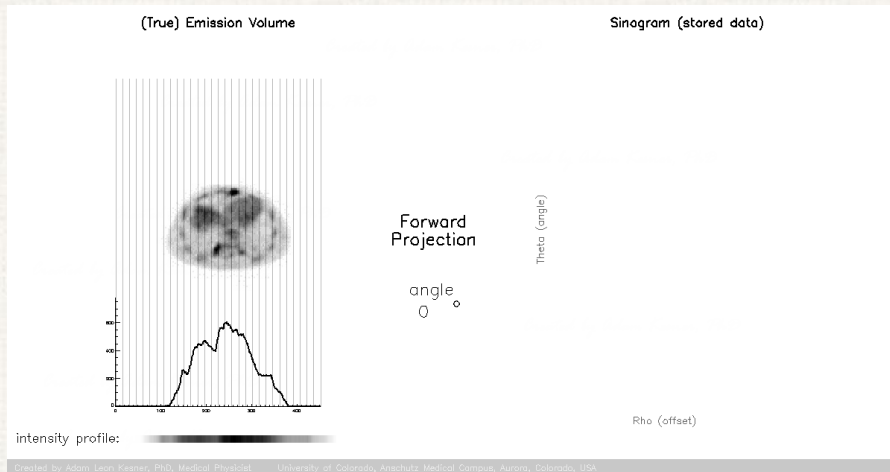*Views from a rotating camera: Sinogram*

Computed 3D Reconstructed Image

Cardiac reversible ischemia: stressed(A), rest(B)

http://www.aipes-eeig.org/white-paper-spect-spect-ct.html

Tomography: Non-invasive Probing of Human Body

(True) Emission Volume — Sinogram (stored data) — Forward Projection — angle 0 — Theta (angle) — Rho (offset) — intensity profile:

Forward Problem:
This is what the imaging system does
$$P = S.V$$

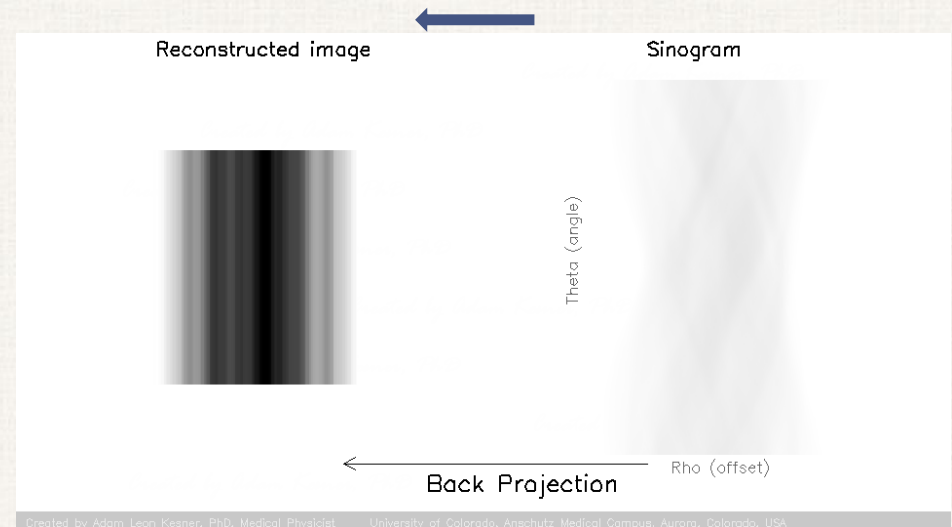*P: Camera Views - input*
S: Camera model / System Matrix - computed
V: Target object - unknown

Reconstructed image — Sinogram — Theta (angle) — Rho (offset) — Back Projection

Inverse Problem:
This is what a reconstruction algorithm does
$$V = S^{-1}.P$$
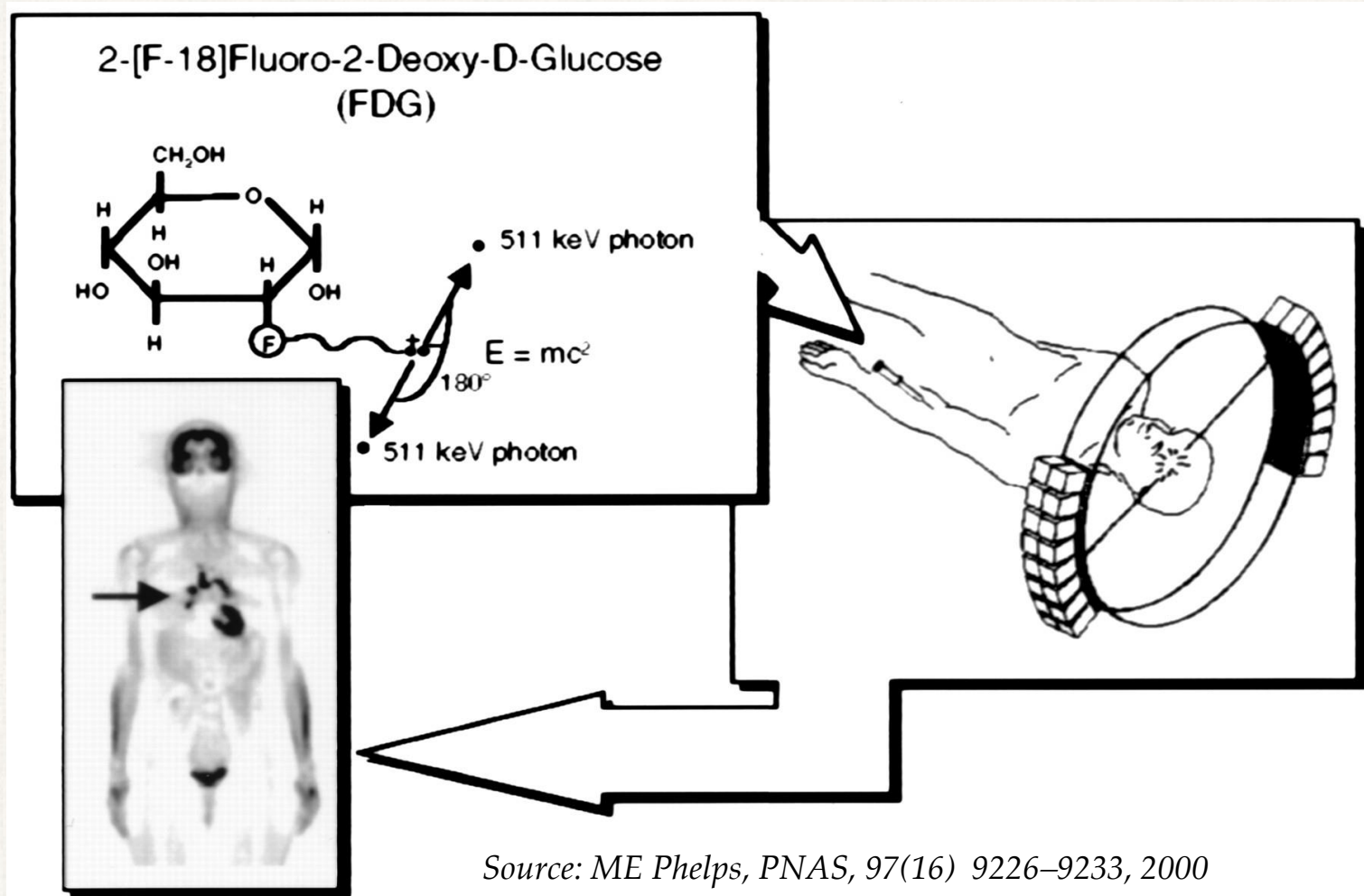
Types of Imaging

- ## Anatomical Imaging
  - o **Where is some organ located?**
  - o **Where is the tumor located?**
  - o **What is the bone density on spine?**

  - o **Example:**
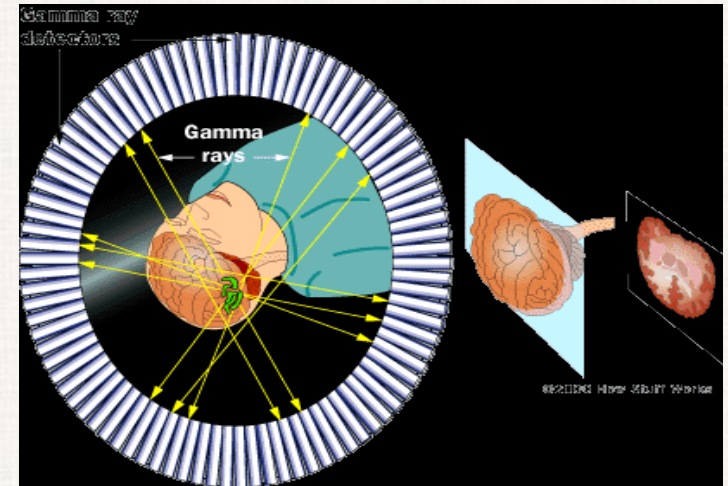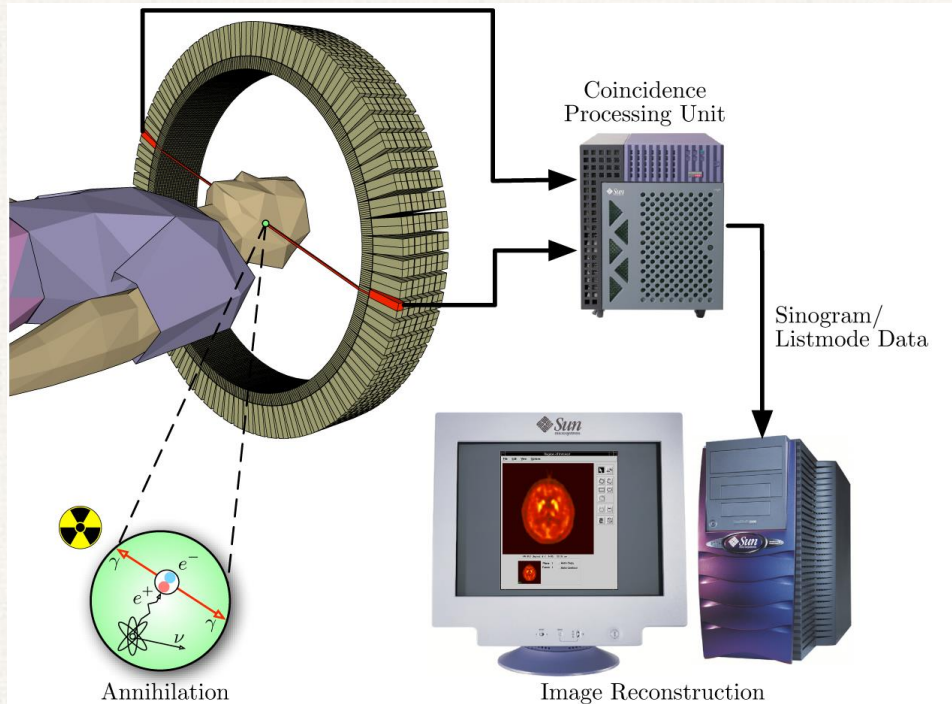   - *Absorption of X-ray: Computed Tomography (CT)*

- ## Functional Imaging
  - o **Where is the targeted physiological function taking place?**
  - o **What is the strength of that function?**
  - o **How are the nerve cells functioning on heart muscles?**

  - o **Example:**
    - *Concentration of probing molecules, which emits gamma rays: Emission Tomography (SPECT and PET)*

Emission Tomography: Functional Imaging

2-[F-18]Fluoro-2-Deoxy-D-Glucose (FDG)

511 keV photon

$E = mc^2$

180°

511 keV photon

Source: ME Phelps, PNAS, 97(16) 9226–9233, 2000

PET: Positron Emission Tomography

- **Positron annihilates with electron**
  ⇒ two gamma photons each at 511 keV leave at180°
- **Coincidence detection ("electronic collimation")**

SPECT: Gamma Emission Tomography
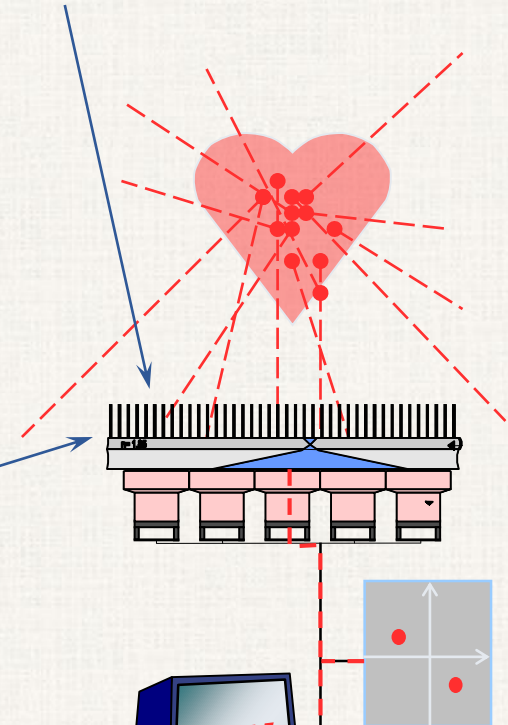
(Single Photon Emission Computed Tomography)

collimators
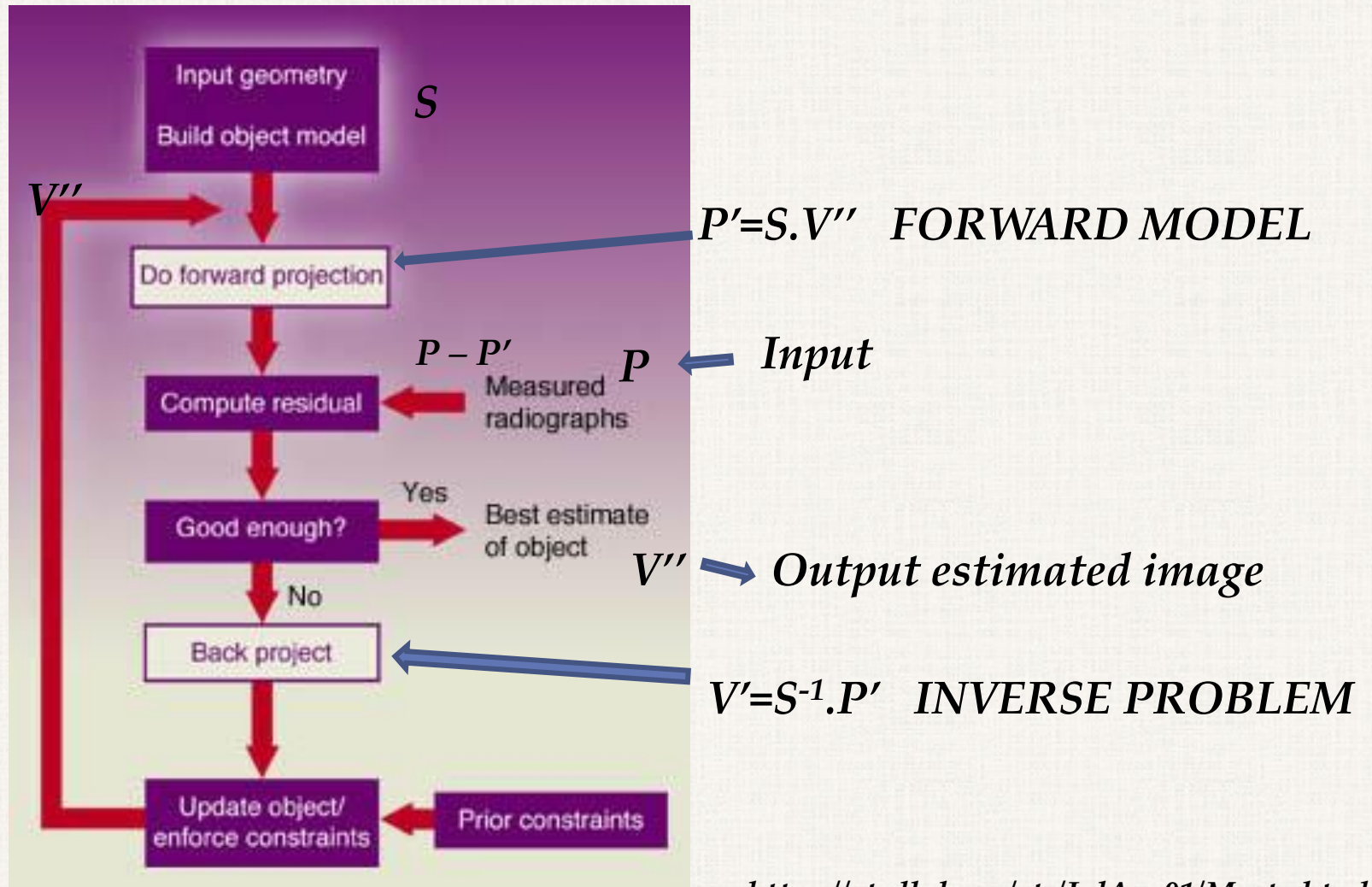
γ-ray detectors

100-200 keV

Resolution

Sensitivity

Acquisition system

X,y

Iterative Reconstruction

S

V''

P'=S.V'' FORWARD MODEL

P – P'

P ← *Input*

V'' → *Output estimated image*

V'=S⁻¹.P' INVERSE PROBLEM

https://str.llnl.gov/str/JulAug01/Martz.html

Dynamic Imaging

- Dynamic Imaging:
  Target Image not stationery during scan
  - e.g. Patient moved

- Dynamic Functional Imaging:
  As the target "function" is taking place:
    - concentration is changing
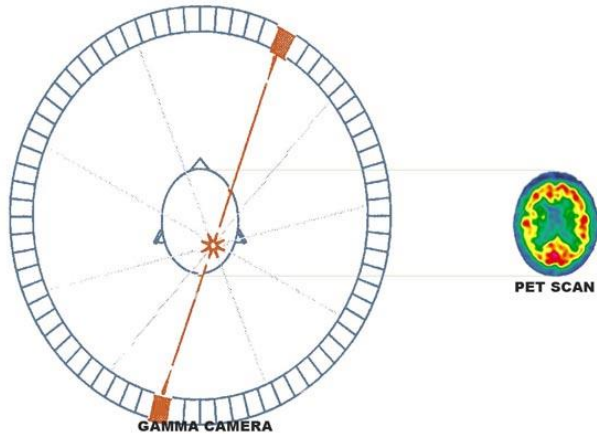   - e.g. nerve cells are picking up norepinephrine

Dynamic Imaging: PET
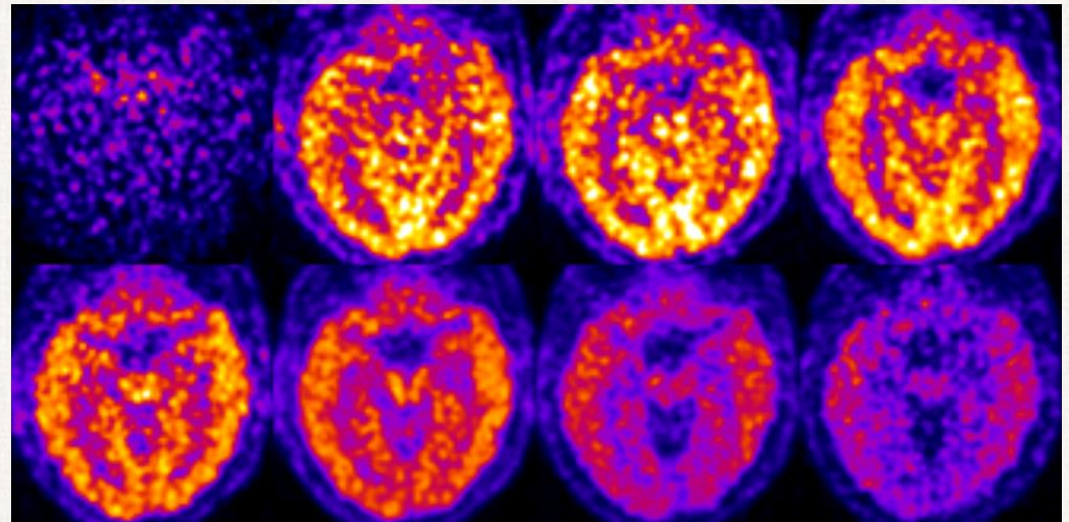## Project 1

3D x t

Dynamic Imaging: PET
Project 1

PET: views from all angles available at all instances.

PIB tracer binding on Alzheimer's studies

- *Time-lapsed Reconstructed 3D images, a slice through human brain*

- *Tracer concentration is changing with time* ➔

Dimensions of the Problem

- **V = 64x64x64 voxels => 262,000 => x4 bytes => 8 Mb**

- **T = 35 snapshots or views => 8 Mb x 35   => 280 Mb**

- **F = 4 target functions**
  - **upstream and downstream blood,**
  - **reference specific tracer binding,**
  - **non-specific binding**

Dynamic PET: Alzheimer's studies

CIFA: Cluster-Initialized Factor Analysis

Input: 4D images of possible Alzheimer's patient
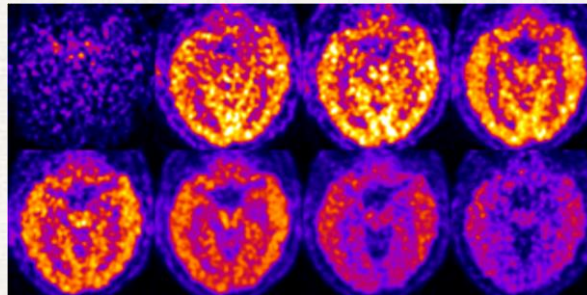
Output: Detect affected tissues based on their tracer dynamics

Boutchko R, Mitra D, Baker S, Jagust W, and Gullberg GT. (April 2015) "Clustering Initiated Factor Analysis (CIFA) Application for Tissue Classification in Dynamic Brain PET." Journal of Cerebral Blood Flow & Metabolism – Nature, doi:10.1038/jcbfm.2015.69.

CIFA Algorithm

Problem: Recognize 3 tissue types by tracer kinetics
Carotid artery, Normal tissue, Alzheimer's affected tissue (PIB attached to beta-amyloid);

$$V_k(t) = \sum_{j=1}^{J} C_{k,j} f_{j,t}$$

f: Time basis functions
C: Coefficients of time
    basis functions
k: voxel index
J: Number of
    time basis functions.

$$arg \min_{C,f} \left\{ \|Cf - V\|^2 + \text{Regularization} \right\}$$

Non-negative matrix factorization (NNMF):
Alternating optimization for C and f

Seung HS, and Lee DD. (1999) "Learning the parts of objects by non-negative factorization." Nature.

CIFA is Cluster-initialized Factor Analysis

NNMF is very sensitive to initialization:
Garbage in garbage out!

R-clustering to initialize NNMF
R-clustering = Representative Clustering
Just find out J number of representatives in data

Input: $\{V\}$ = N time series (TS) V^n of length K each, the elements are denoted as V^n_k

Output: P TS C^p_k, each representing a cluster

1. **Find the ensemble average M^A of all V^n;**

// the first cluster is farthest from average

2. **Find a fixed number J of TS in $\{V\}$ that are furthest from M^A, denote those as set $\{F_1\}$;**

3. C^1 = **average of $\{F_1\}$;**

4. **For p =2 through P**

5.   **Find a fixed number J of TS in $\{V\}$ that are furthest from all C^l, $l \in \{1,P\text{-}1\}$, denote those as set $\{F_p\}$;**

6. C^p = **average TS of $\{F_p\}$;** // *end for;*

// refine clusters to be furthest from each other:

7. **Repeat the loop 4-6, only this time the set $\{F_p\}$ denotes J TS that are furthest away from all C^l, $l \in \{\{1,P\}$ excluding $p\}$.**
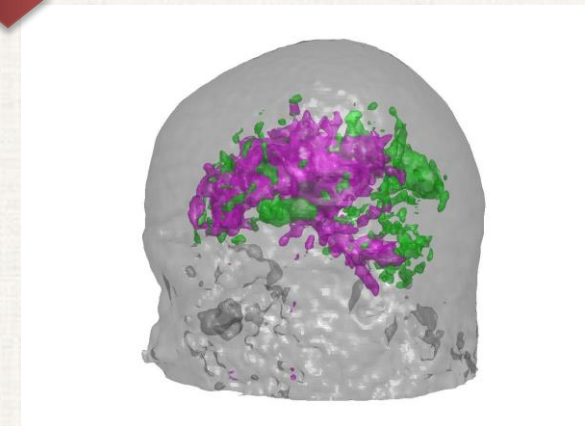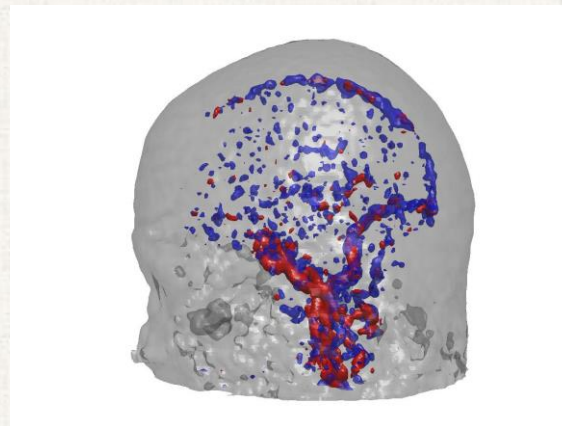
Results from CIFA on Alzheimer's studies

R-clustering on raw data
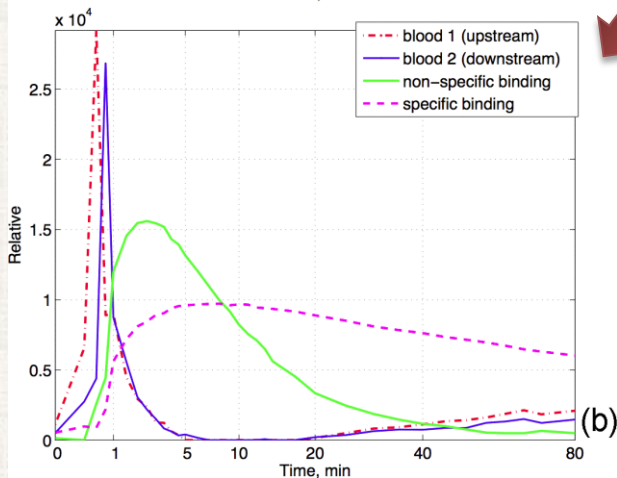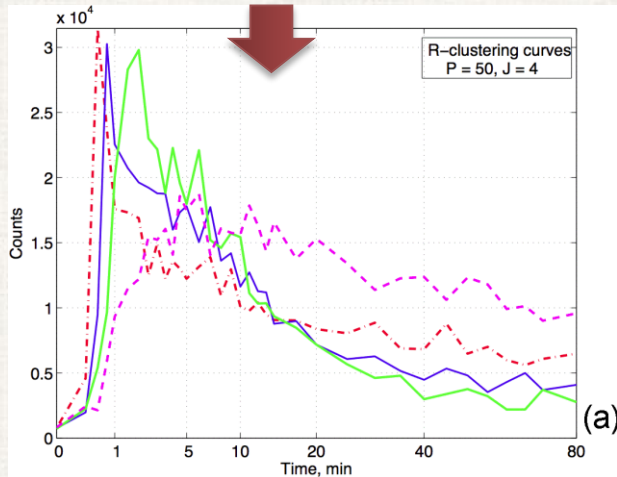
Output 1: Time-activity curves (or f) for:
i) Carotid artery, ii) Veins, iii) Normal tissue, and
iv) Alzheimer's affected tissue (PIB attached to
β-amyloid)

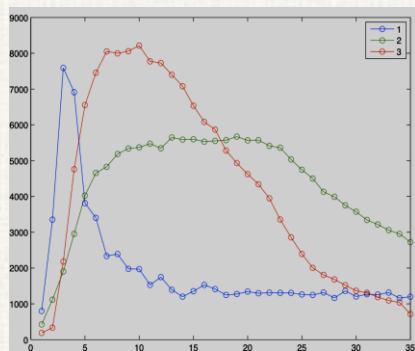*Output 2: 3D views of Corresponding segments*
(coefficients C)

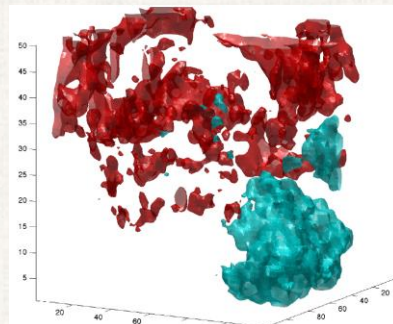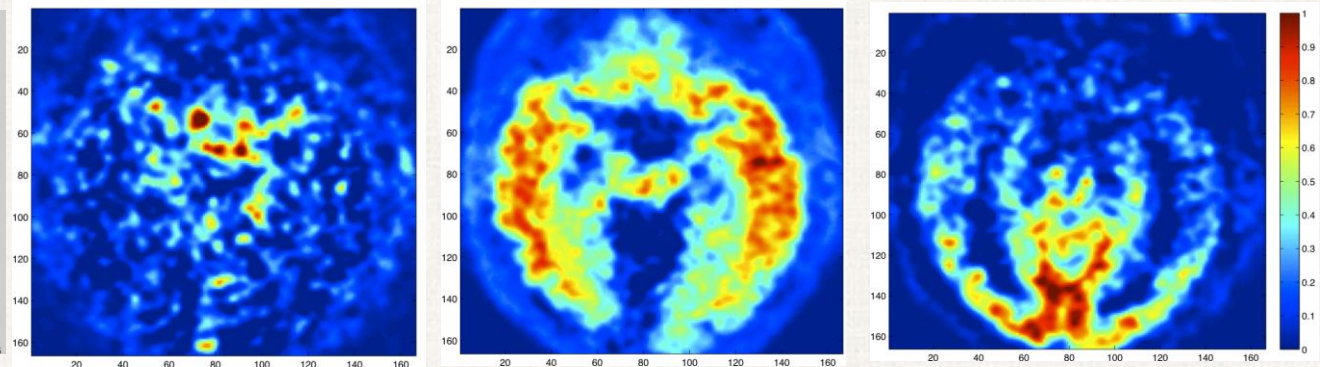# Results from CIFA on Alzheimer's studies

Question: Recognize 3 tissue types by tracer kinetics
i) Carotid artery and vein, ii) Normal tissue,
iii) Alzheimer's affected tissue (PIB attached to beta-amyloid);

Output 1: Time-activity curves

Output 2: Corresponding segments

3D view of above tissues

Dynamic Imaging: SPECT

Project 2

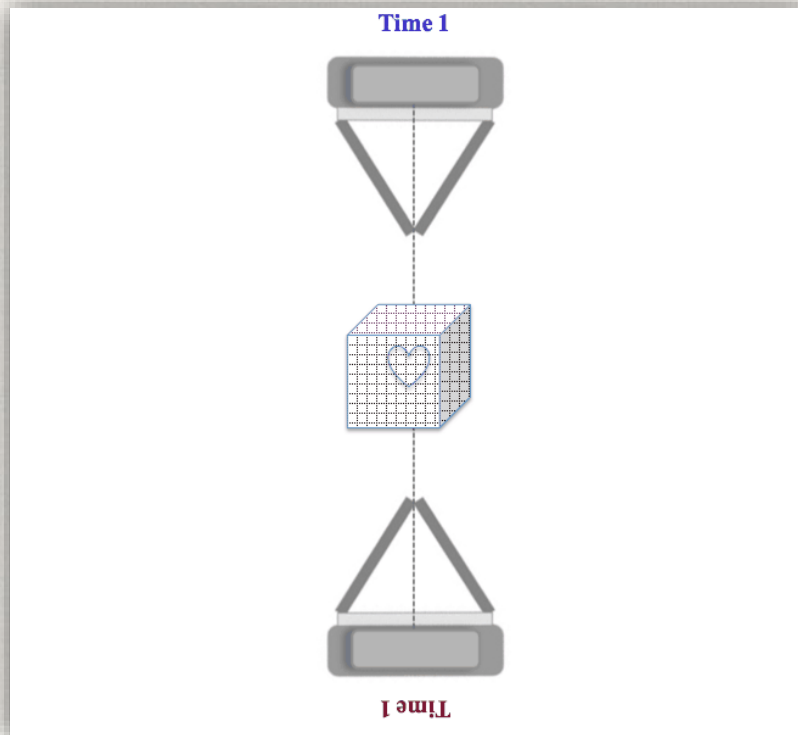$$2D \times \theta \times t$$

Dynamic Data with SPECT

blood pool

heart muscle
(myocardium)

other organs
(E.g., liver)

Time activity curves (TACs)

blood

heart

liver
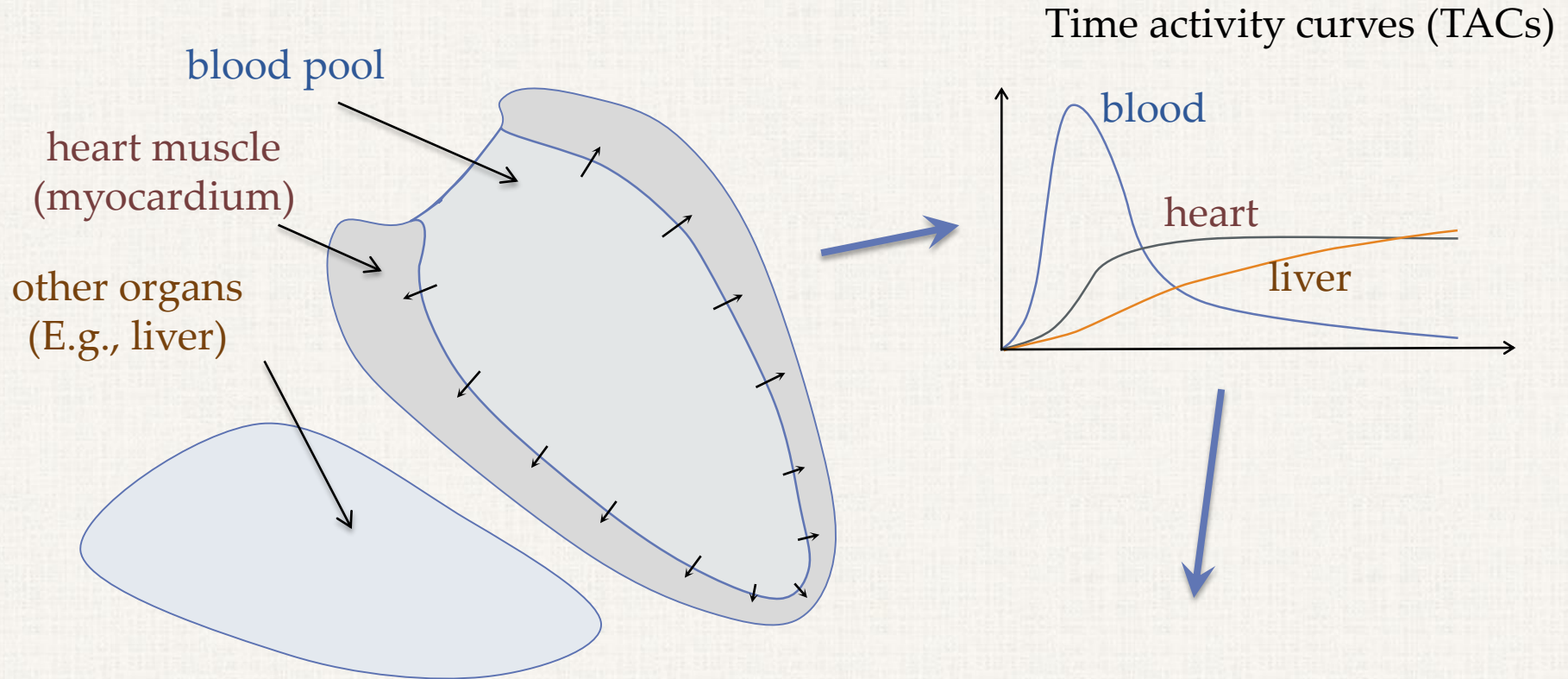
Local tracer exchange (kinetic) rates –
important diagnostic parameters

Dynamic Imaging: SPECT
Project 2

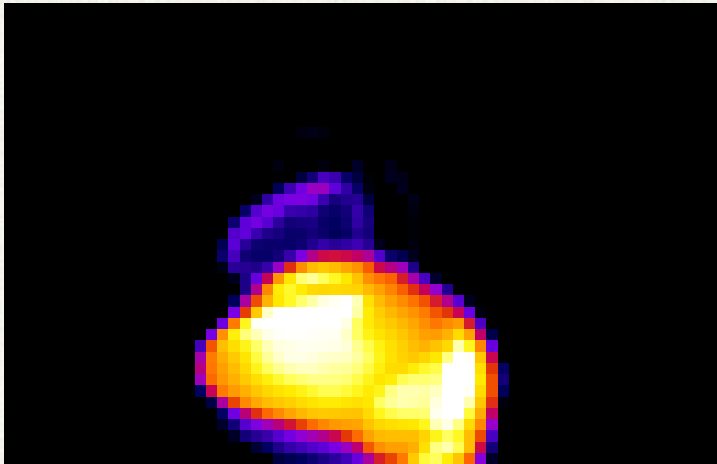Only two projections for each time point: more difficult than PET

First Rotation Sinogram Immediately after injection
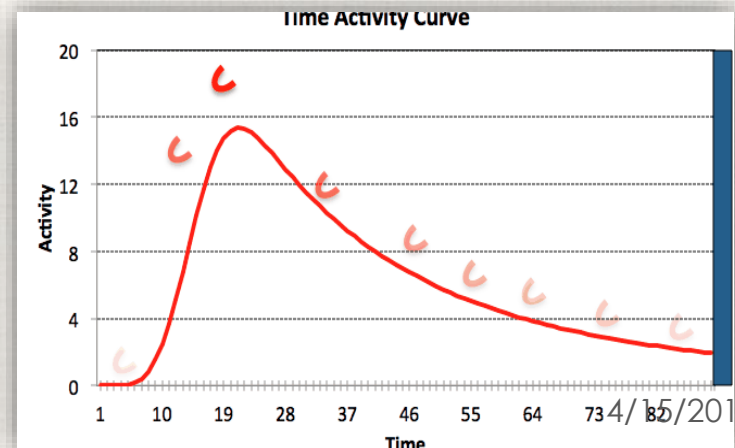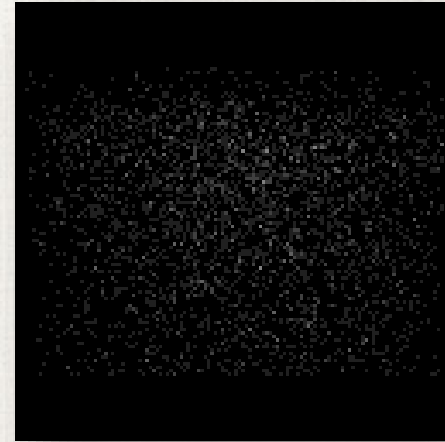
Dynamic Vs. Static Projections

Static Sinogram

Dynamic Sinogram

SPECT Dynamic Imaging- Challenges

- Ill-posed Problem
  - *less time for data acquisition on each view*
  - *Low counts – high noise*

- Underdetermined Problem
  - *Fewer data in each time window after binning*
  - *Inconsistent sinogram*

- Small animal imaging:
  - Low resolution & motion

Dimensions of the Problem

- V = 64x64x64 voxels => 262,000 => x4 bytes => 8 Mb

- P = 64x64 pixels per view   x   120 views => 500,000
                                                   => x4 b => 20 Mb

- System matrix, S = 8 x 20 => 160 Mb
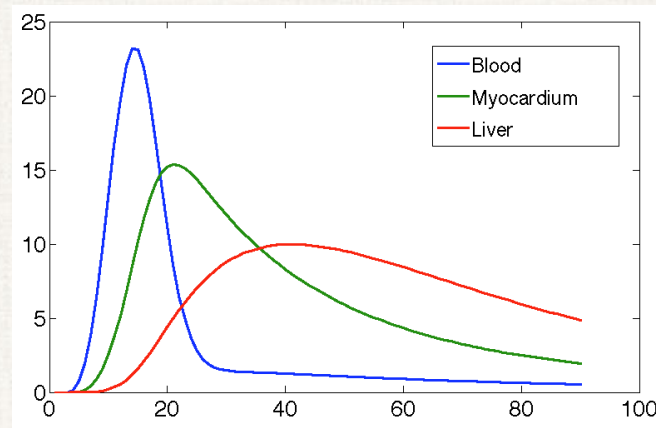
- F, target functions = 3 to 4

Dynamic SPECT: Task

- *Goal*: Estimation of tracer's **temporal** distribution in the imaged tissues *directly* from inconsistent projections

Input: Dynamic Sinogram
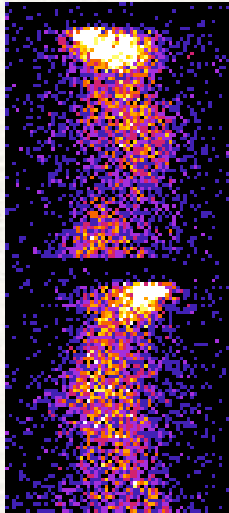
Output: Time Activity Curves (TACs)

Dynamic SPECT Model

- Dynamic SPECT is modeled by:

- 4D volume is factored with J time basis functions:

$$P_n(t) = \sum_{k=1}^{K} S_{n,k} V_k(t)$$

$$V_k(t) = \sum_{j=1}^{J} C_{k,j} f_{j,t}$$

$$P_n(t) = \sum_{k=1}^{K} S_{n,k} \sum_{j=1}^{J} C_{k,j} f_{j,t} \longrightarrow P = SCf$$

Space   Time

P: Sinogram as function of time
S: System Matrix
V: 4D Imaged volume, as function of time.
n: pixel index on the detector
k: voxel index on the volume

f: Time basis functions
C: Coefficients of time basis functions
J: Number of time basis functions.

Static Image Reconstruction

- **Optimize for V:**

$$arg\min_{V}\left\{\|SV-P\|^2_w + \text{Regularization}\right\}$$

Existing Dynamic SPECT Image Reconstruction Methods

- ## Spectral Methods:
  - Select a set of representative time basis functions (Typically cubic b-splines) and optimize for coefficients.

    Problem: what is the best set of basis functions?

$$arg \min_{c} \left\{ \|SCf - P\|^2_w + \text{Regularization} \right\}$$

- ## Factor Analysis of Dynamic Structures (FADS):
  - Initialize and optimize both time basis functions and coefficients.

    Problem: what to initialize with?

$$arg \min_{c,f} \left\{ \|SCf - P\|^2_w + \text{Regularization} \right\}$$

Our Approach: Spline-initialized FADS (SIFADS)

Enhancements:

- o Combined those two types of optimization
- o Imposed Data-driven Prior information as constraints in optimization

Consequence:

Reduced dependence on initialization

Abdalah M, Boutchko R, Mitra D, and Gullberg GT. "Reconstruction of 4-D Dynamic SPECT Images From Inconsistent Projections Using a Spline Initialized FADS Algorithm (SIFADS)." IEEE Transactions in Medical Imaging, 34(1): 216-228, 2015.

Innovation 1– Hybrid Optimization

- Spline-Initialized FADS (**SIFADS**) algorithm

Spectral Estimation
> 1. Estimate initial TACs using spectral method

Initial Guess Preparation
> 2. Using segmented static volume, average TACs of each segment

FADS Refinement
> 3. Initialize FADS with those averaged curves

Innovation 2- Impose Prior information

- Reconstruction of later frames is segmented
- Segments are used to impose regularization functions:

1. **An anisotropic total variation** $\Theta(C) = |ATV(C)|_1$
2. **Coefficients mix prevention** $W(C) = |\vec{C_j} \cdot \vec{C_i}|_1$ *j≠i*
3. **Curves' smoothness constraint** $F(f) = |\nabla f|_1$

$$arg\min\left\{\|SCf - p\|_w^2 + \lambda_1 Q(c) + \lambda_2 W(C) + \lambda_3 F(f)\right\}$$

Spatial Regularization   Temporal Regularization

Innovation 2– Masking

Static Volume

Currently Estimated Coefficients

Segment

Threshold

Segmented Static Volume M^s

Masked Coefficients M^d

Intersection

$\cap$

Unrecognized Regions
$$\omega = M^d - M^s \cap M^d$$

Recognized Regions $= M^s \cap M^d$

1

2

3

ω
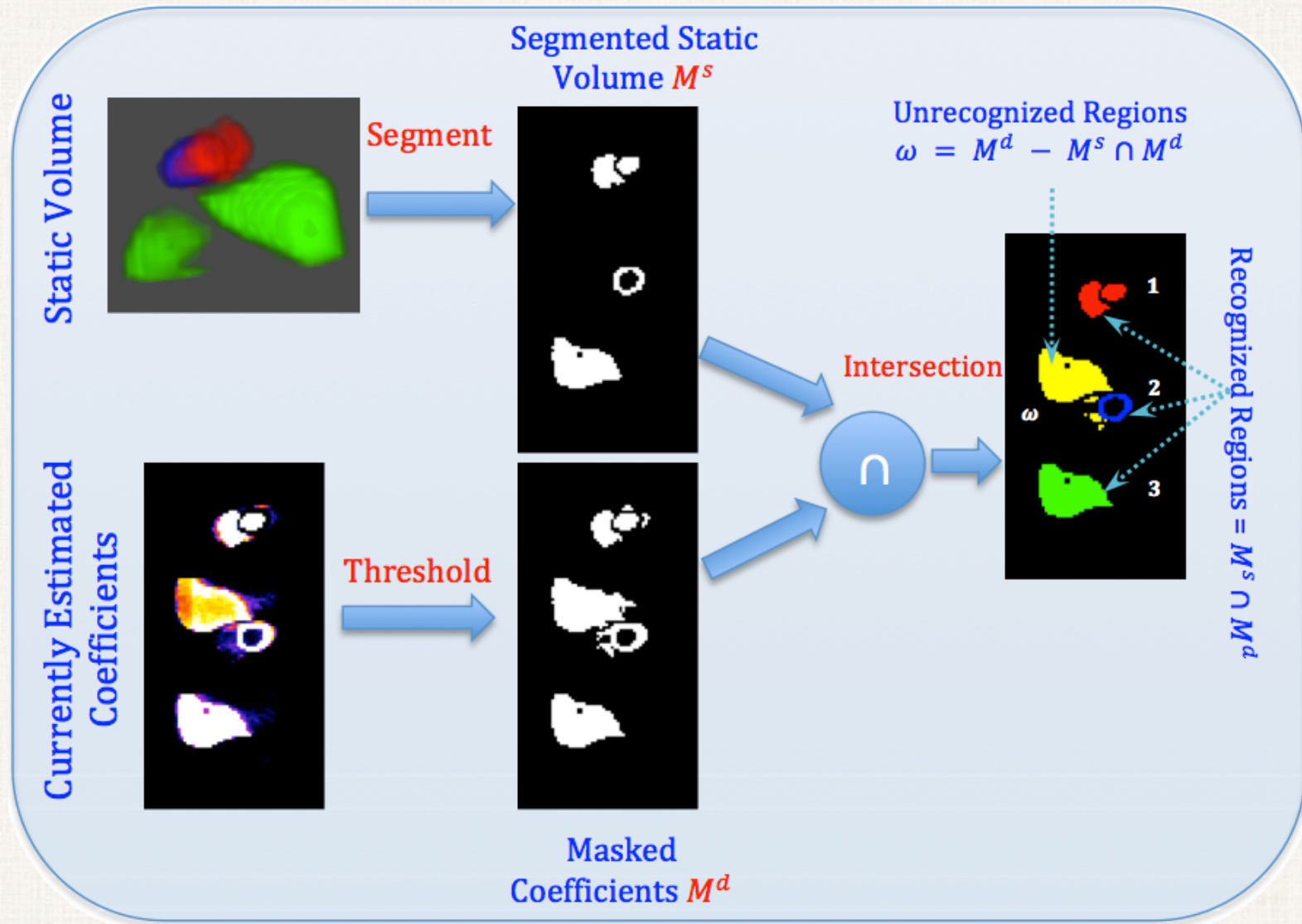
Innovation 3– Data-driven dynamic update of Regularization Parameters

$$arg\min\left\{\|SCf - p\|_w^2 + \lambda_1 Q(c) + \lambda_2 W(C) + \lambda_3 F(f)\right\}$$

- Weighting parameters are dynamically updated at each iteration by:

$$\lambda_1^{[k+1]} \underline{=} \frac{1}{g^{[k]}} \frac{\|SC^{[k]}f^{[k]} - p\|_w^2}{Q(c^{[k]})}$$

$$\lambda_2^{[k+1]} \underline{=} \frac{1}{g^{[k]}} \frac{\|SC^{[k]}f^{[k]} - p\|_w^2}{W(c^{[k]})}$$

$$\lambda_3^{[k+1]} \underline{=} \frac{1}{g^{[k]}} \frac{\|SC^{[k]}f^{[k]} - p\|_w^2}{F(f^{[k]})}$$

- Where $\gamma^{[k]}$ is estimated by:

$$g^{[k]} = g_0 \sqrt[4]{\frac{\|SC^{[k]}f^{[k]} - p\|_w^2}{0.05 \times \|p\|_w^2}}$$

I. Kazufumi et. al., 2011.

SIFADS Algorithm

SIFADS Algorithm

Spectral Estimation

//STEP 1: Initialization:

    //B-Splines fitting

1:   $f^0 \leftarrow \{B - Spline\,functions\}$;

2:   $C^0 \leftarrow 0$;

3:   $C^1 \leftarrow arg\min_c \left\{\left\|SC^0 f^0 - p\right\|_w^2\right\}$

Initial Guess Preparation

    // Estimating initial Curves and Coefficients:

4:   $V(t) \leftarrow C^1 f^0$;

5:   $f^1 \leftarrow Ave(segment(V(t))$;

6:   $C^2 \leftarrow arg\min_c \left\{\left\|SC^1 f^1 - p\right\|_w^2 + \lambda_1\Theta(C^1) + \lambda_2\Omega(C^1) + \lambda_3\Phi(f^1)\right\}$

// STEP 2: FADS Refinement

FADS Refinement

7:   $(C^*, f^*) \leftarrow arg\min_c \left\{\left\|SC^2 f^1 - p\right\|_w^2 + \lambda_1\Theta(C^2) + \lambda_2\Omega(C^2) + \lambda_3\Phi(f^1)\right\}$

    // Estimate and Output Final Curves:

8:   $V(t) \leftarrow C^* f^*$;

9:   $f \leftarrow Ave(segment(V(t))$;

MAP Algorithm for coefficients estimation

$C \leftarrow 1$;

for i = 1 to **N** do

   $U(C^{[i]}) \leftarrow \lambda_1\Omega(C^{[i]}) + \lambda_2\Theta(C^{[i]})$;

   $\nabla U(C^{[i]}) \leftarrow \frac{\partial U}{\partial C^{[i]}}$;

   $C^{[i+1]} = \frac{C^{[i]}}{\sum Sf + \nabla U(C^{[i]})} \sum \frac{P}{\sum SC^{[i]} f} Sf$;

end for

return C

MAP Algorithm for coefficients and factors estimation

for i = 1 to **N** do

   // Coefficient minimization:

   $U_1(C^{[i]}) \leftarrow \lambda_1\Omega(C^{[i]}) + \lambda_2\Theta(C^{[i]})$;

   $\nabla U_1(C^{[i]}) \leftarrow \frac{\partial U_1}{\partial C^{[i]}}$;

   $C^{[i+1]} = \frac{C^{[i]}}{\sum Sf^{[i]} + \nabla U_1(C^{[i]})} \sum \frac{P}{\sum SC^{[i]} f^{[i]}} Sf^{[i]}$;

   // Factor minimization:

   $U_2(f^{[i]}) \leftarrow \lambda_3\Phi(f^{[i]})$;

   $\nabla U_2(f^{[i]}) \leftarrow \frac{\partial U_2}{\partial f^{[i]}}$;

   $f^{[i+1]} = \frac{f^{[i]}}{\sum SC^{[i+1]} + \nabla U_2(f^{[i]})} \sum \frac{P}{\sum SC^{[i+1]} f^{[i]}} SC^{[i+1]}$;

end for

return C, f

Validation with Simulation

Coefficients used for simulation
(NCAT phantom)
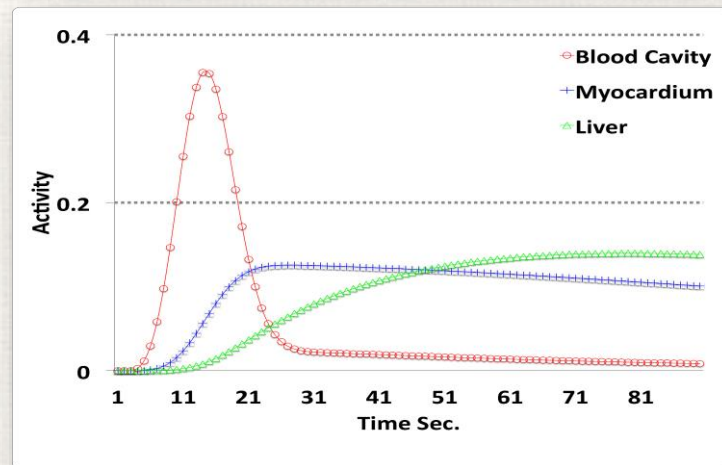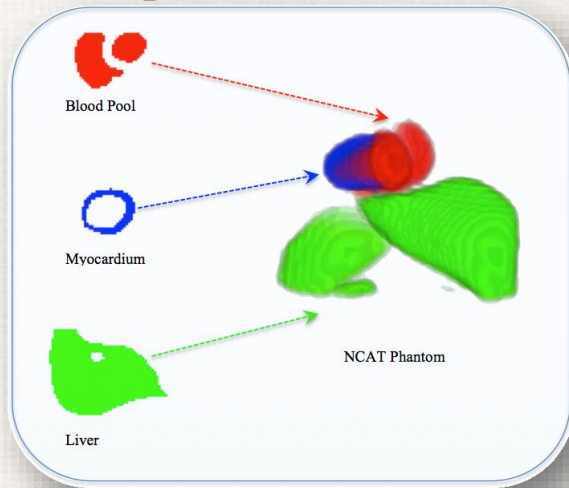
Generated projections with Poisson noise
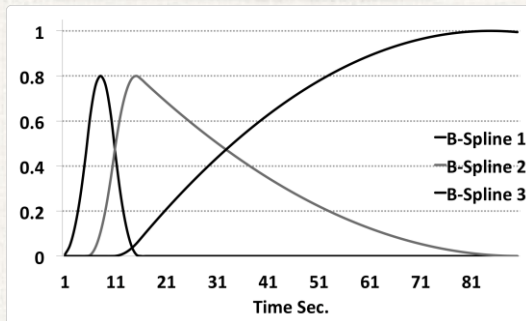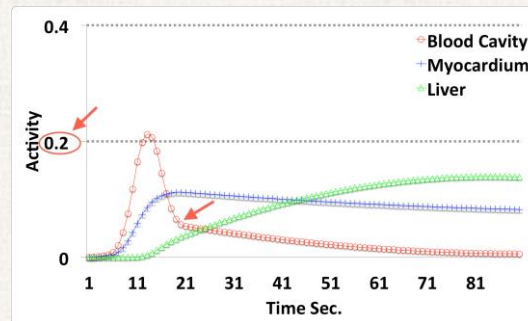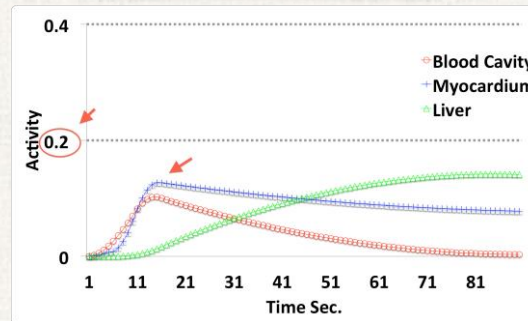

0   20   40

Time Sec.
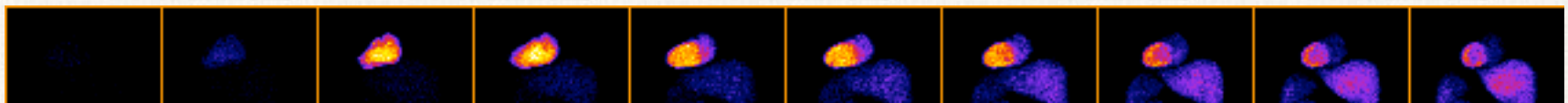
Results: Drawback of Pure Spline-method

B-splines
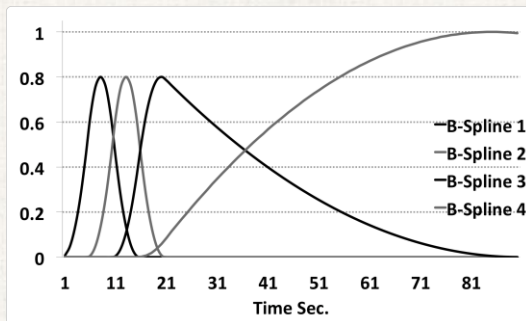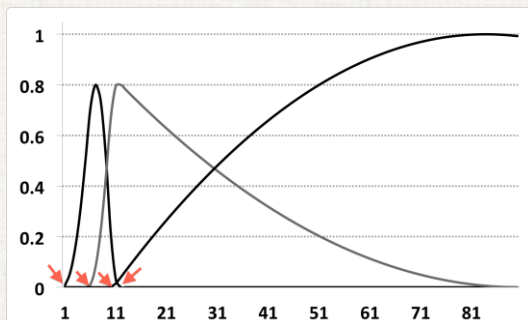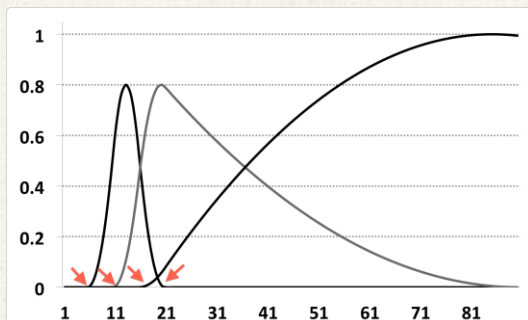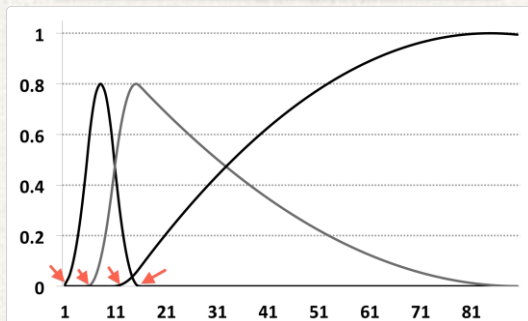
Spectral

Ground truth for Simulation
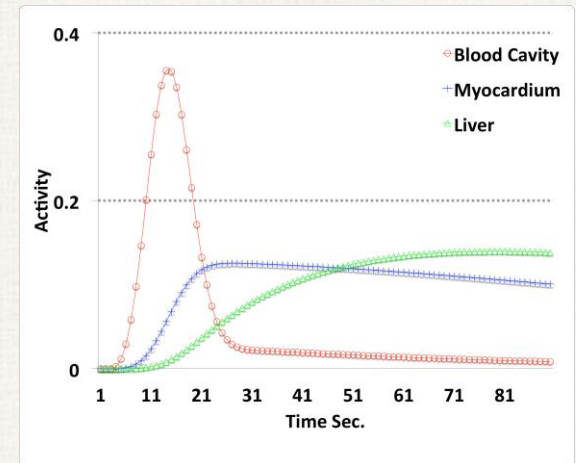
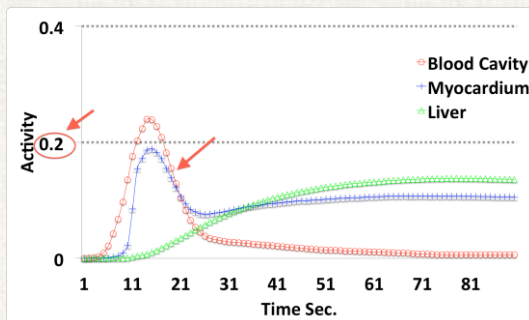$$arg\min_{c}\left\{\left\|SCf - p\right\|_{w}^{2}\right\}$$

Drawback:
Very sensitive to initial time basis function
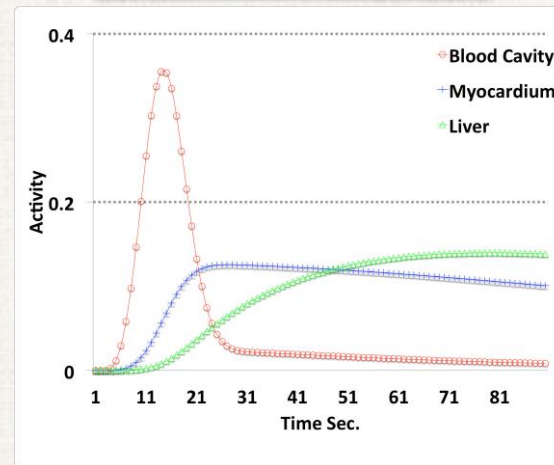
Results: Drawback of Arbitrarily Initialized FADS-method

Initial Functions

FADS
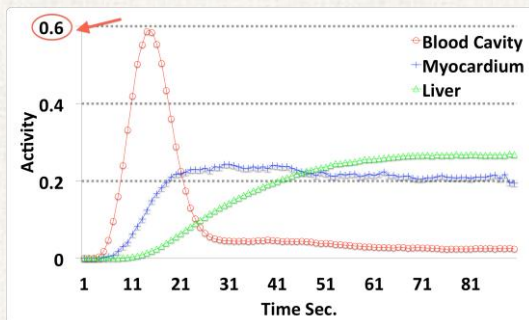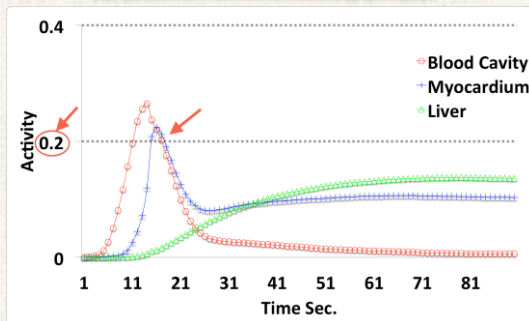
Ground truth

$$arg\min_{c,f}\left\{\left\|SCf - p\right\|_w^2 + \text{Reg}\right\}$$

Drawback:
Very sensitive to
initialization
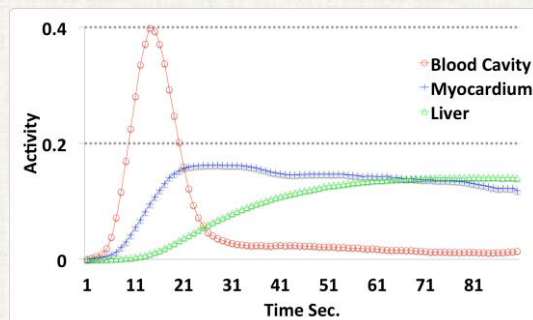
Spline vs. SIFADS results
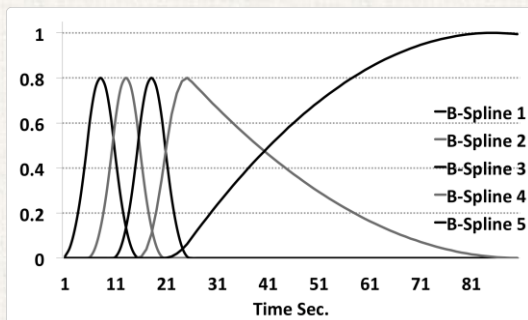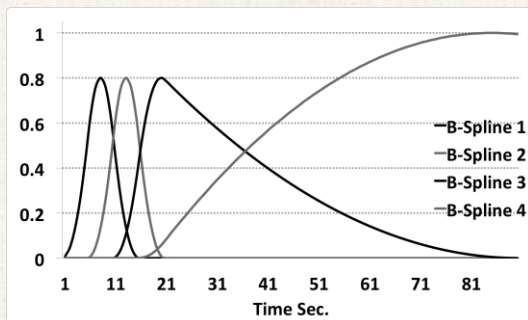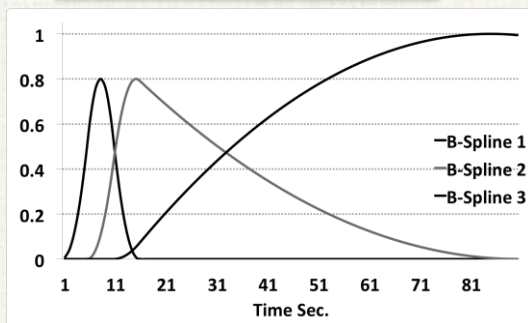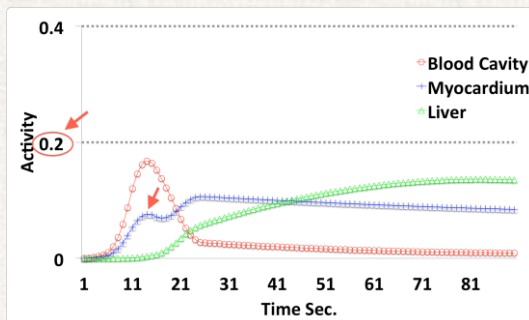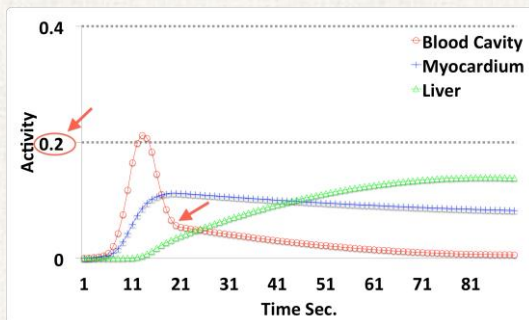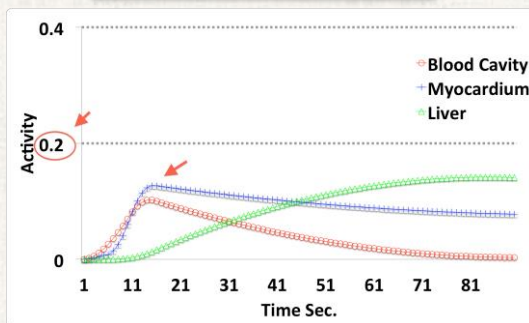
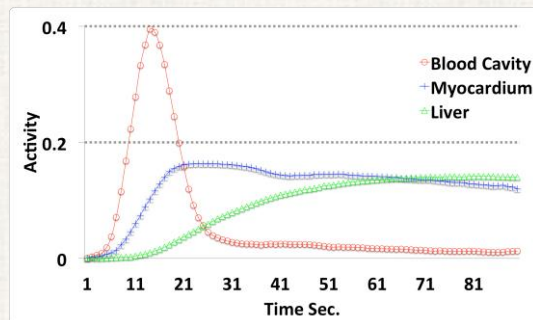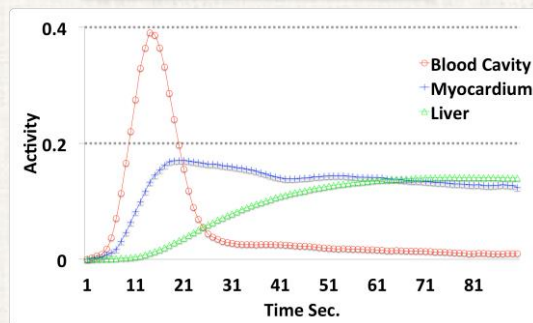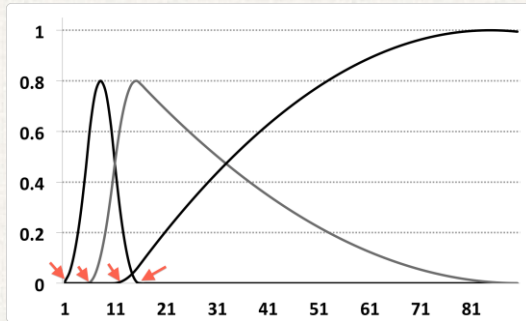# FADS vs. SIFADS Results
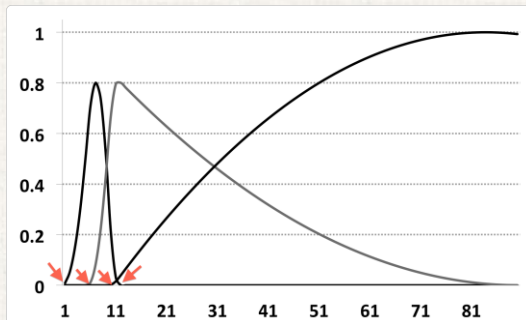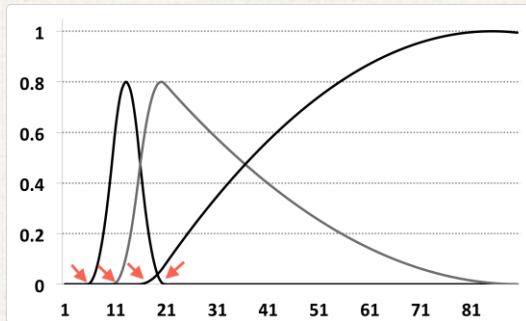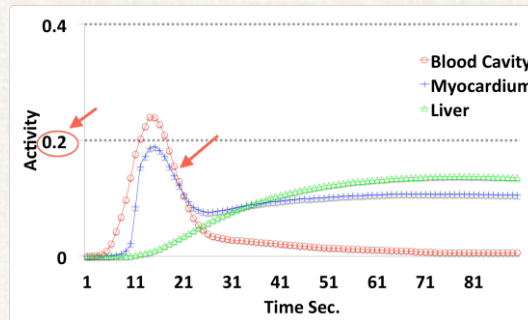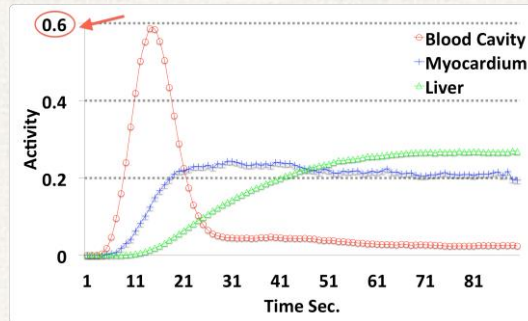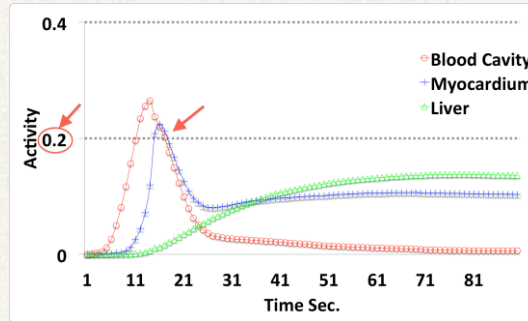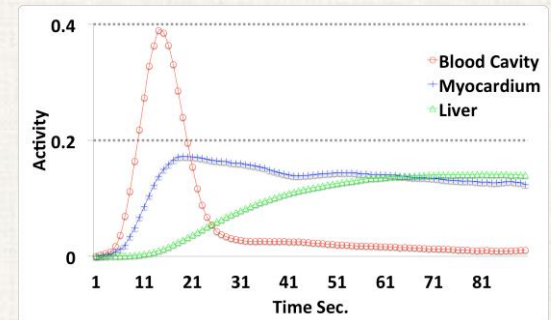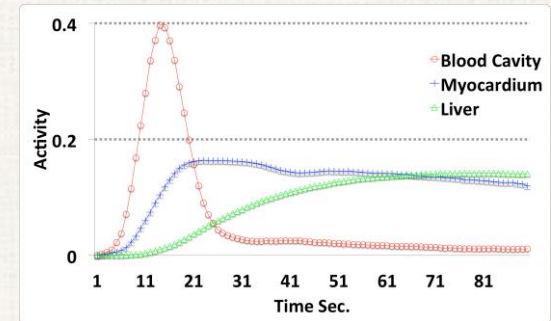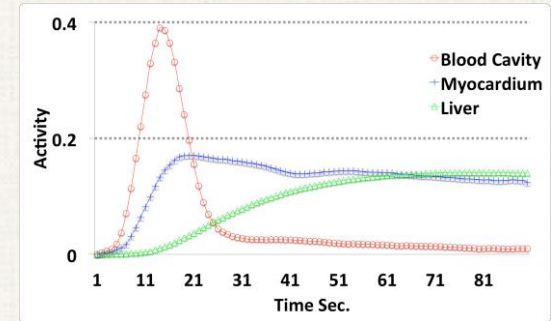
Real Data: Rat heart

- Dynamic, pinhole SPECT study, rat's heart
- Collimators:1.5×2 mm tungsten pinholes
- GE VG3 Millennium Hawkeye camera
- Acquisition started with injection of 7 mCi ^{123}I-MIBG
- 30 rotations, 90 one-second views, per rotation
- Detector pixel: 4.42 mm, recon voxel 0.8 mm

Results from the Rat Study

Original projections:

Estimated rat TACs from the first inconsistent rotation:

Estimated projections by forward projecting dynamic reconstruction:
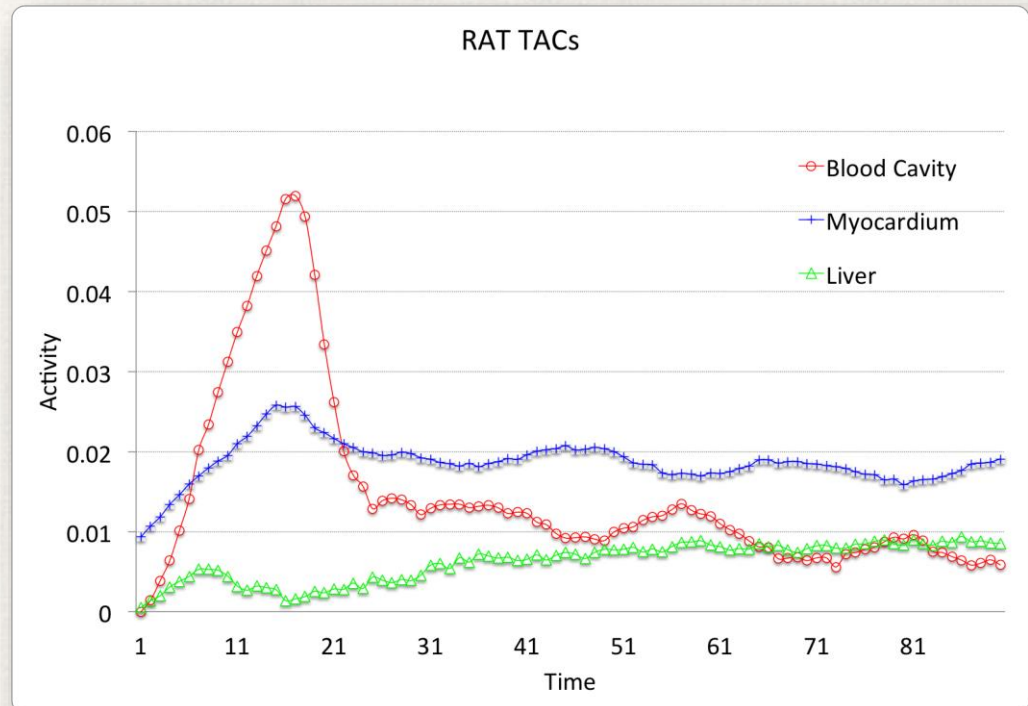
Results from a Canine Study

- GE Millennium VG3Hawkeye SPECT/CT camera
- Two detectors, H-mode, parallel LEHC collimators, 4.42 mm pixel resolution
- ^{99m}Tc-teboroxine stress study of a canine subject
- 24 rotations, 72 one-second views per rotation
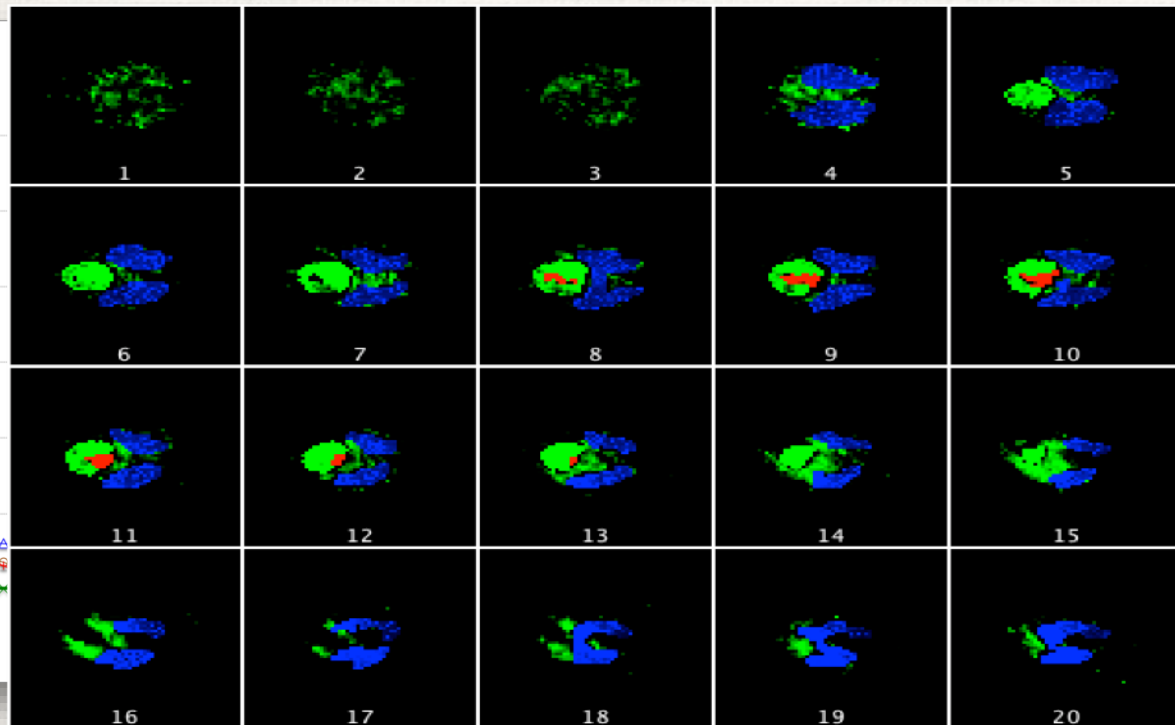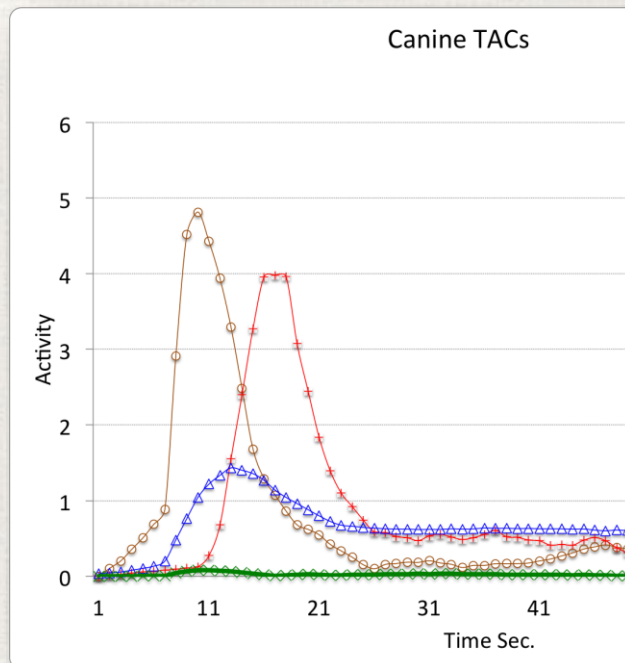
Summary on SIFADS

- Segmentation according to TACs

- Several regularization functions proposed and imposed using anatomical information.

- Hybrid optimization procedure (SIFADS) developed to reduce the initialization issue

- *TACs as a new biomarker?*

Primal-Dual (PD) Optimization - to improve efficiency: Canine study

MLEM
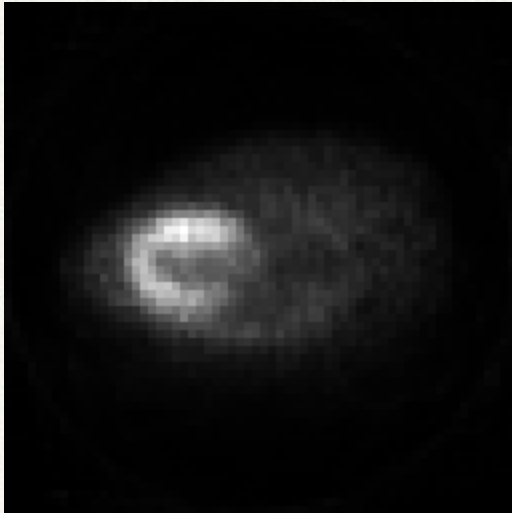
Conjugate Gradient
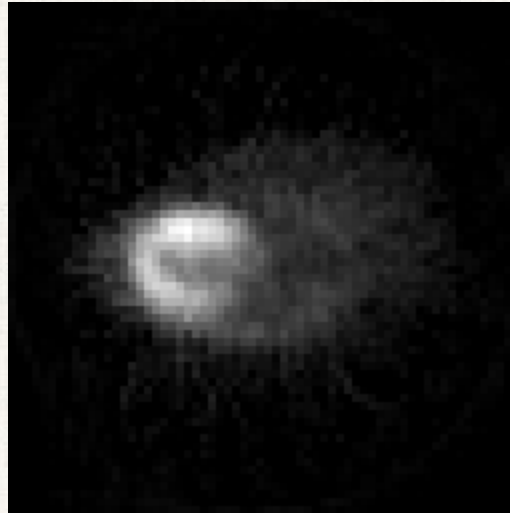
PD
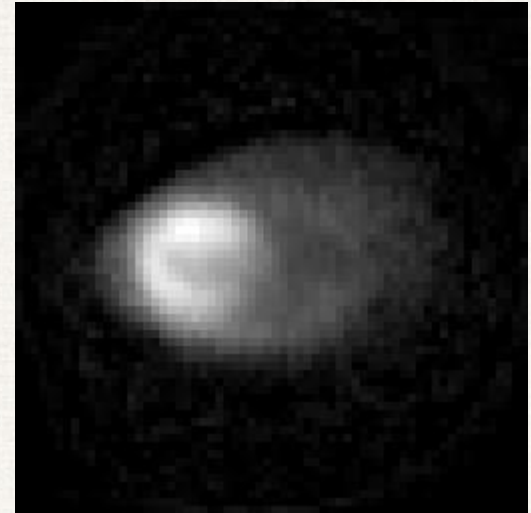
Convergence:

MLEM convergence

CG convergence

PD gap

Chen S, Pan H, Abdalah M, Boutchko R, Mitra D, and Gullberg GT. (2014)
"Image reconstruction with a primal–dual algorithm," SNMMI, Seattle, Washington
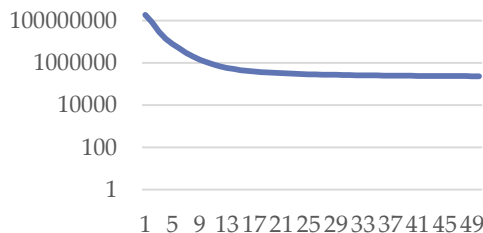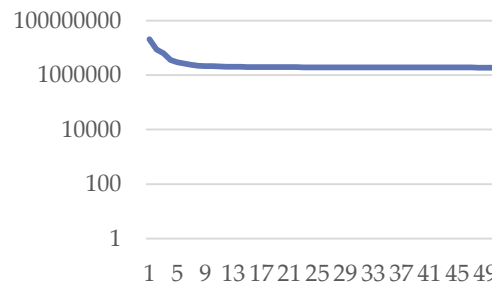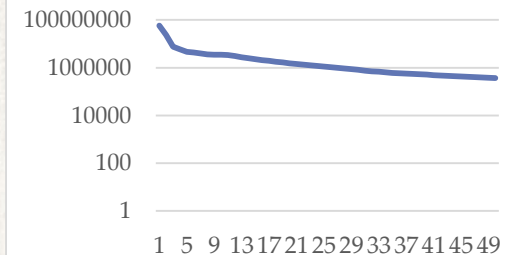
Cell Tracking on Fluorescent Microscopy

Project 3

2D x t

Cell Tracking on Fluorescent Microscopy

Project 3

FRET: Fluorescence Resonance Energy Transfer
New Technology for quantifying gene expression in live single cells

Fig. I.

TRENDS in Cell Biology
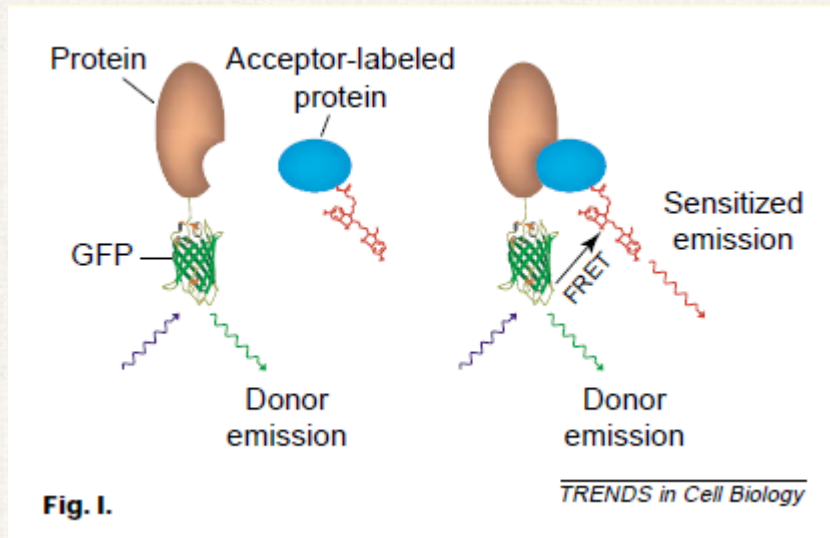
$$E_A(i) = \frac{F^{DA}(i) - F^D(i) \cdot R_D - F^A(i) \cdot R_E}{F^A(i)}$$

Three channels for each Time-frame:
Donor emission (F^D), Acceptor Emission (F^A), D-to-A Excitation emission (F^{DA})

"Imaging biochemistry inside cells"
TRENDS in Cell Biology, 11(5): 203-211, 2011
Wouters, Verveer and Bastiaens

Cell Tracking on Fluorescent Microscopy
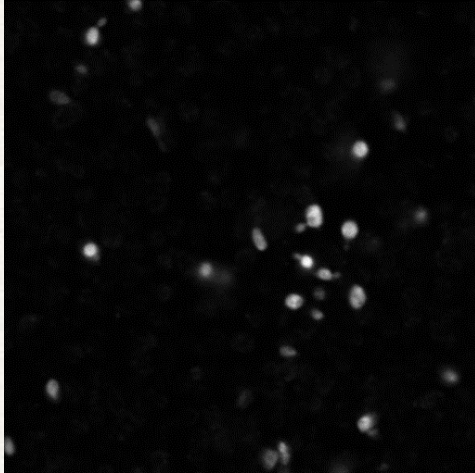
Project 3

Input:
Frames of the time-lapsed 2D image from a confocal microscope
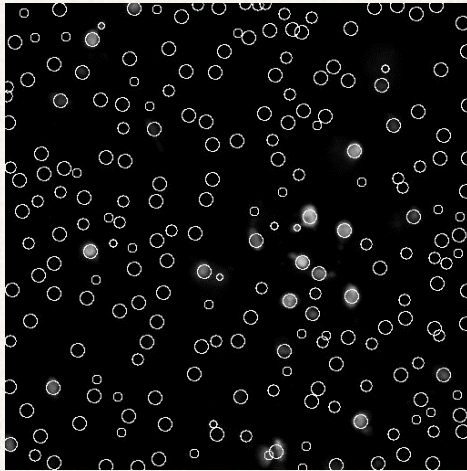
Output:
Same frames after tracking by scale-space segmentation

Cell Tracking on Fluorescent Microscopy

Project 3
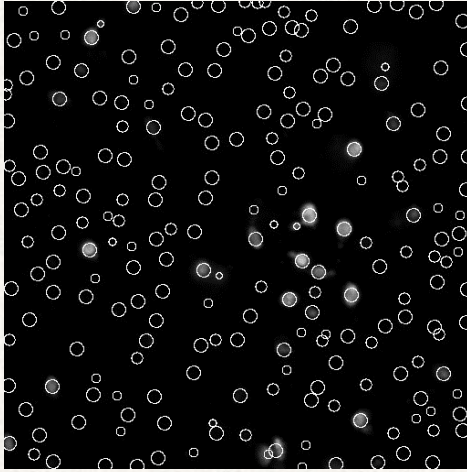
Scale Space Algorithm:
    Handles varying sizes of cells

Problems:
    Live cells move in 3D – across the frame,
        in-out of focal plane;
            cells also divide!

    How to track a cell from frame to frame?

Semi-solved ("threading"):
    Search around a cell in next frame for similar average intensity

Cell Tracking on Fluorescent Microscopy

Project 3
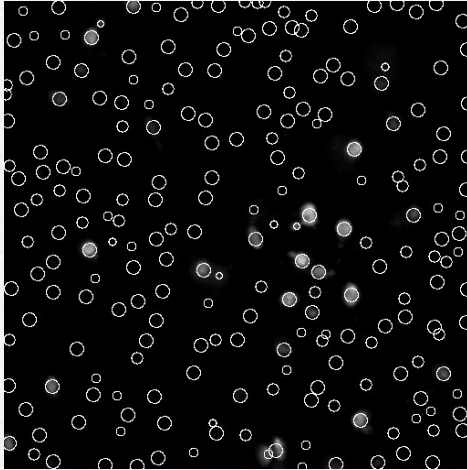
Tracking a cell from frame to frame by threading algorithm
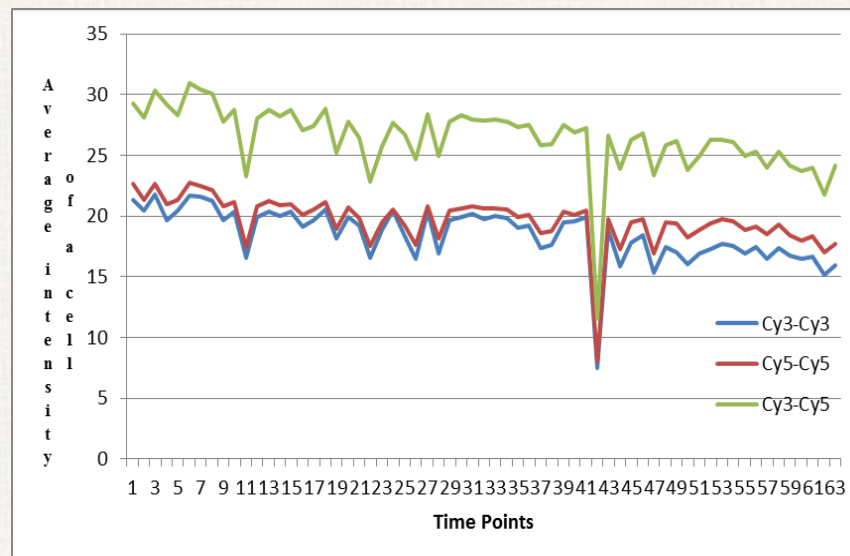
A sample cell's average intensity variation over time-lapsed frames.
Three colored curves represent three channels:
Cy3 excitation-Cy3 emission, Cy5 excitation-Cy5 emission, and Cy3 excitation-Cy5 emission.

Rigid Motion in SPECT Projections

Project 4

Conventional Perfusion studies with Static Imaging:
Step and shoot mode, consistent projection, but patient moves during scan
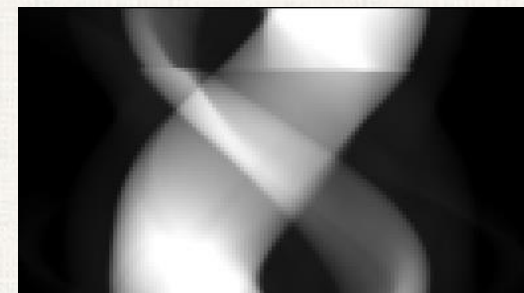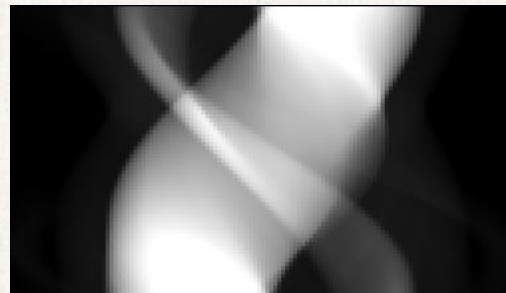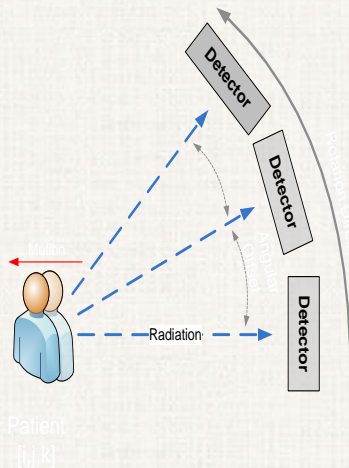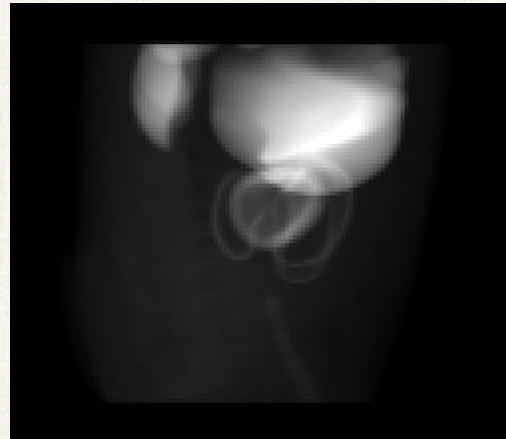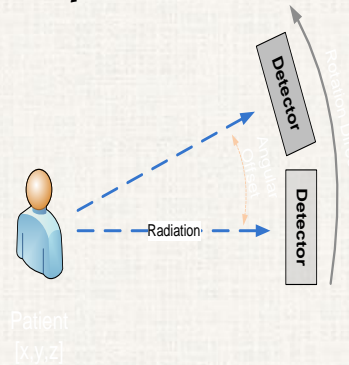
Motionless Dataset   **Motion-Corrupted Dataset**

Corrections for motion with *SinoCor*

Before Correction   **After Correction**

Motion between projections:
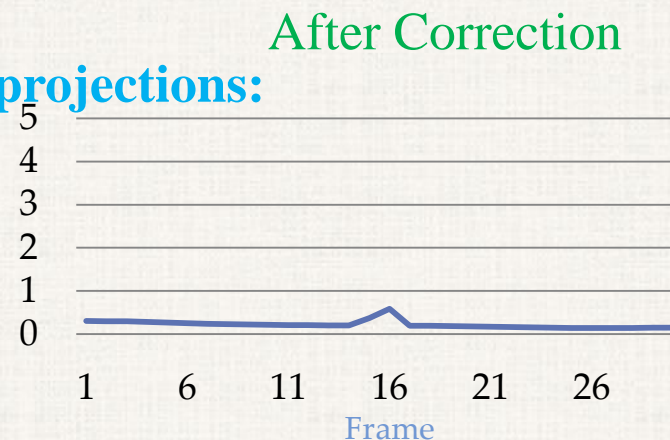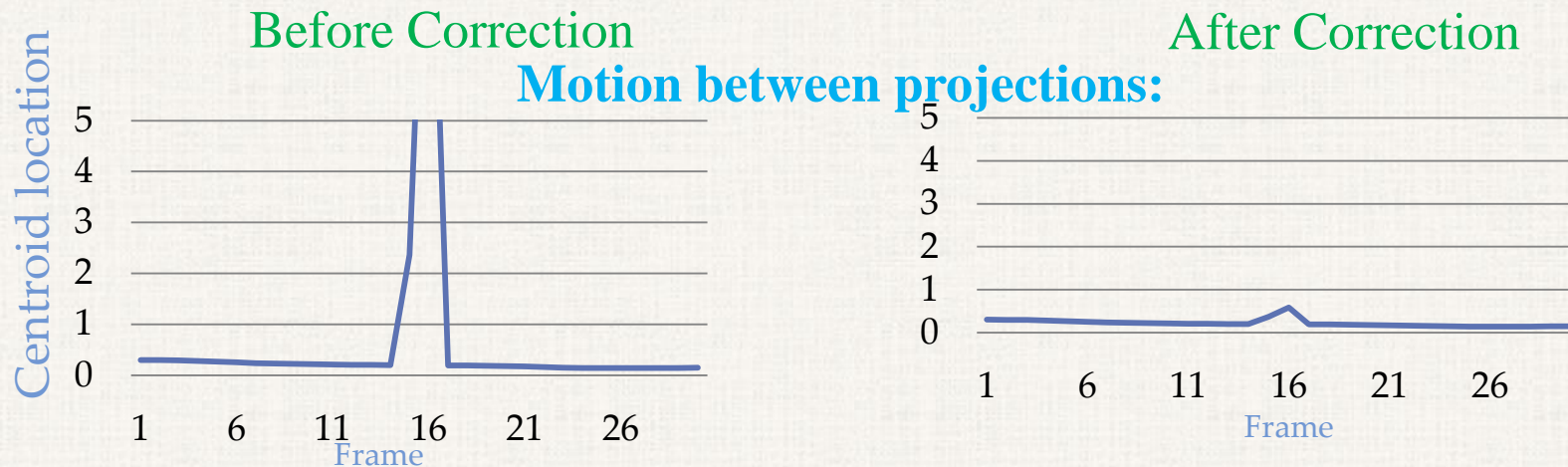
Blurring on a projection:
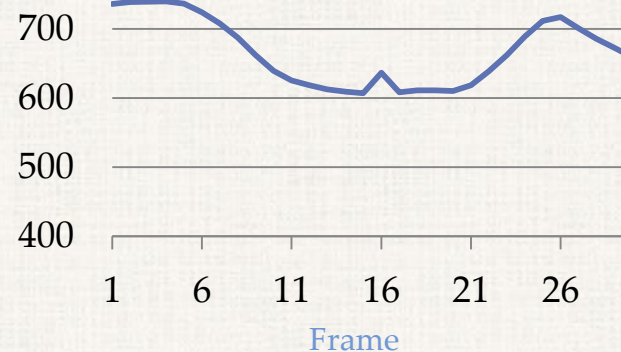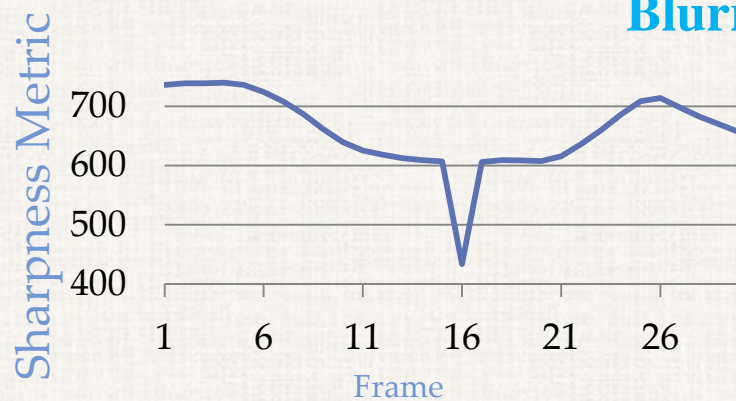
Eiland D, Mitra D, Abdalah M, Butchko R, and Gullberg GT. (2012)
"SinoCor: Inter-frame and Intra-frame motion correction tool,"
Conf. Record IEEE Nuclear Science Symposium and Medical Imaging Conference, Anaheim, CA.

Moffitt Cancer Center

Future

- **Improving Algorithm:**
  - Optimization (Primal-Dual)
  - Parallelization (using High-performance Computing)
  - Removing Manual Intervention: Automatic Segmentation for Masking
  - Better basis function (Spline-Wavelet)
  - Motion compensation
    - Rigid motion of patient (*SinoCor*)
    - Beating heart (Blind deconvolution)
    - Respiratory motion (Rank optimization)

- **Multiple-modality data-fusion for better reconstruction in both**
  - Machine learning (Cross-modality reconstruction with prior knowledge infusion across different modalities)
  - Data management to keep track of metadata across modalities (Research Medical Imaging database: ReMI.lbl.gov)

Imaging Beyond Medicine:
Problems with similar mathematics -

Linear Algebra, Statistics, Numerical Optimization, ...

<u>*Spread the cost of imaging research across multiple agencies*</u>

- *Muon tomography:*
  cosmic ray-generated muon scattered from heavy metals

- *Cosmology:*
  Structure of universe from telescopic observations

- *Electron Microscopy:*
  3D view of a virus or molecule, & in action

- *Seismic:*
  Acoustic waves from earthquake or artificial source to study subsurface structure & activities

Quantifying nuclear threats with muon tomography algorithms

Kim Day

Faculty Advisor: Dr. Debasis Mitra, Dept. of Computer Science, Florida Institute of Technology

Abstract

The Florida Tech High Energy Physics Group A led by Dr. Marcus Hohlmann has been developing a prototype muon tomography station (MTS) for identifying shielded nuclear materials. The MTS typically requires days of data taking in order to reconstruct objects. Since waiting for days will not be an option in practical use, this study focused on developing algorithms that could work with small amounts of data for identifying suspect materials. Focus was put on finding "clear" areas that did not contain high density materials. The algorithm was able to identify a 2cm block of uranium in the prototype station within an hour's worth of data.

Motivation

- Millions of packages enter the US every day, but only a small percentage can be scanned without slowing down the process.
- Nuclear material smuggling can be easily done by using lead shielding to hide the radiation.
- There is a need for a method that can see through lead shielding without being intrusive or time consuming.

About muon tomography

- Muon tomography is a 3D visualization method that uses naturally occurring muon showers to reconstruct objects.
- When a muon passes through a dense material, it will scatter slightly in its trajectory.
- A muon tomography station (MTS) can record the incoming and outgoing paths of all the muons that pass through it.
- The point of scattering can be found by finding where the incoming and outgoing rays intersect.
- Analyzing the high-angle scattered points will show where the densest materials are.
- A prototype cubic foot detector has been built at Florida Tech (figure 1).

Algorithm description

- The algorithm divides the volume inside the station into an array of voxels (3D pixels). Then, it counts the number of straight muon tracks that pass through each voxel.
- Since muons will pass straight through clear areas without scattering, voxels that contain a high straight track count are more likely to be clear of nuclear material.
- Scattered tracks were also used to show which voxels contained scattered points (less likely to be clear).
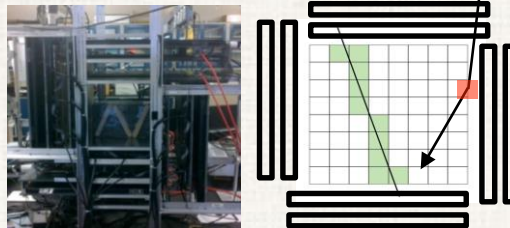

Figure 1 (left): The Florida Tech prototype cubic foot muon tomography station (left)
Figure 2 (right): Visualization of the voxel grid inside the station. The green voxels are more likely to be clear since a straight track passes through them, while the red voxel is less likely since it contains a scattering point.

Sources

US Customs and Border Protection cargo security
http://www.cbp.gov/border-security/ports-entry/cargo-security
Los Alamos initial research paper on muon tomography
http://scienceandglobalsecurity.org/archive/sgs16morris.pdf

Findings

- Tested on the "5 target" scenario: an arrangement of five 2cm blocks of different densities (figure 3).
- Able to see high density materials ($Z >= 50$) with 1 hour's worth of data taking (6000 tracks, figure 4).
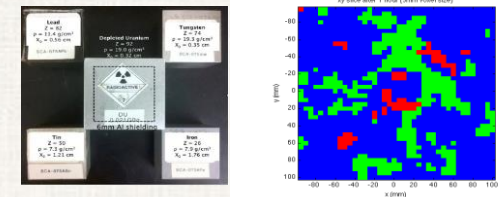- Taking data for 2-3 hours (12000/18000 tracks, figures 5-6) allowed for visualizing the shapes of the blocks.

Figure 3 (left): The "5 target" arrangement of 2 cm blocks (lead, tungsten, tin, iron, and uranium).
Figure 4 (right): 2D output of the algorithm showing a horizontal slice through the center of the blocks after 1 hour. Red = threat, green = clear, blue = unknown.
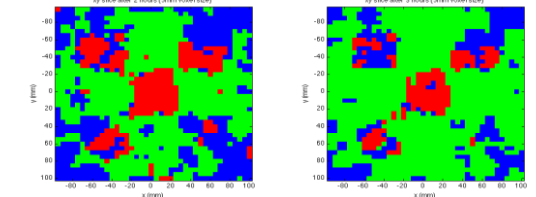
Figures 5 & 6: Output of the algorithm using 2 hours (left) & 3 hours (right) of data.

Conclusion

The clearing algorithm developed for this project was able to identify high density blocks and narrow down much of the search area using 1 hour of data. This is promising for practical use, although the algorithm still requires work on noise reduction and parallelization for increasing the analysis speed.

Debasis Mitra, Computer Science, Florida Tech, dmitra@cs.fit.edu

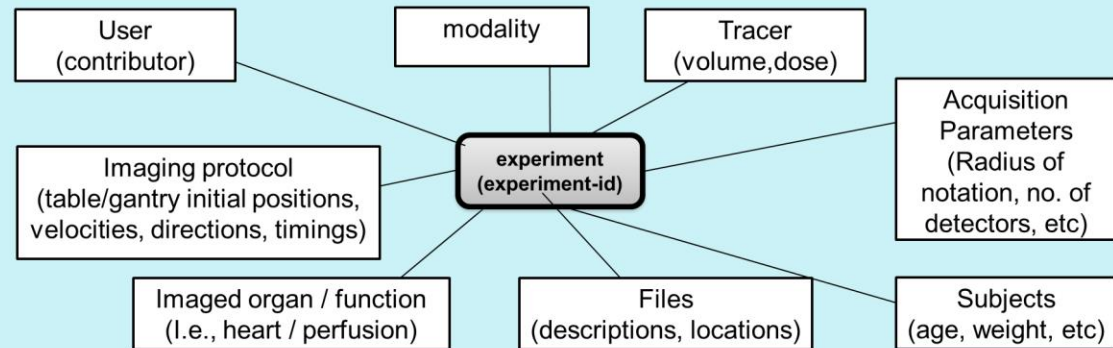# Data Management for Raw Acquisition Data: remi.lbl.gov

RELATIONAL META-DATABASE

Metadata Structure
- information on imaging technology and protocol
- information about subject
- data source information
- content specifications
- Core Entity: Experiment

User (contributor) — modality — Tracer (volume, dose) — Acquisition Parameters (Radius of notation, no. of detectors, etc) — Imaging protocol (table/gantry initial positions, velocities, directions, timings) — experiment (experiment-id) — Imaged organ / function (I.e., heart / perfusion) — Files (descriptions, locations) — Subjects (age, weight, etc)

System
Architecture

Client — Web Browser (JavaScript) — Apache (Passenger) — Server: Rails & Ruby (Active Model) — MySQL Meta-Database — File Storage
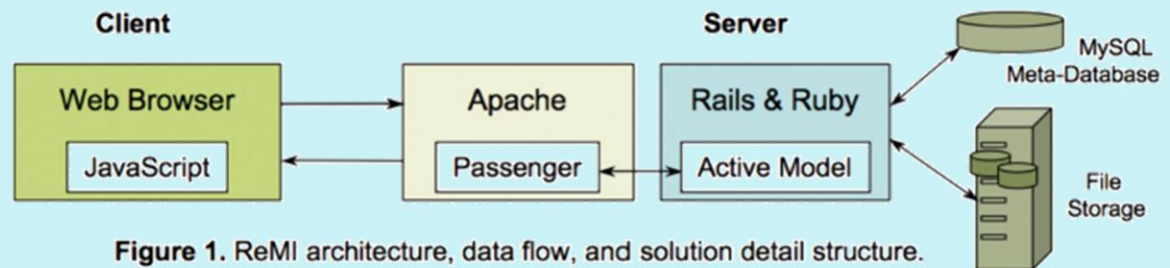
Figure 1. ReMI architecture, data flow, and solution detail structure.

Privacy and Security
- all patient-identifying data are removed before the upload
- upload only by registered users using secured protocols

# Improving Efficiency with GPU: MLEM with Simulation data

256² x 60 SPECT sinogram with 1 pinhole	Ray tracing (sec)	Average per iteration (sec)	Average forward projection (sec)	Average back projection (sec)	Total reconstruction (sec)	Normalized-mean-sqr difference: CPU to GPU images
CPU	2.13	5.91286	1.95625	2.8691	1188.41	
GPU	0.529756	0.286561	0.0951198	0.110944	60.1003	
Ratio CPU/GPU	4.02	20.633	20.56617	25.86	19.773	1.67
128² x 60 SPECT sinogram with 4 pinholes						
CPU	7.34	3.979	1.564	2.044	49.51	
GPU	0.797533	0.0920357	0.0426326	0.0474005	4.01172	
Ratio CPU/GPU	9.203	43.233	36.685	43.121	12.341	1.65
128² x 600 CT sinogram						
CPU	5.32	33.1364	10.169	19.081	340.79	
GPU	0.415884	0.818518	0.306646	0.477997	26.88	
Ratio CPU/GPU	12.792	40.483	33.16	39.9186	12.678	1.57

Reducing communication with CPU improves speed
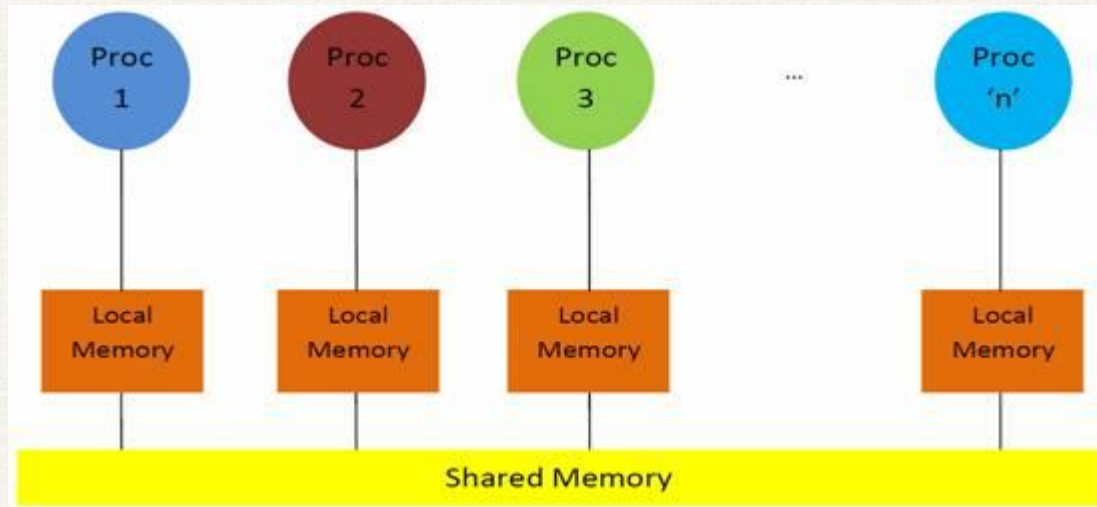
Reorganizing data over local memory has further improved a reconstruction time from 30.55 sec to 24.84 sec

We plan further improvement by holding more data longer time on local memory
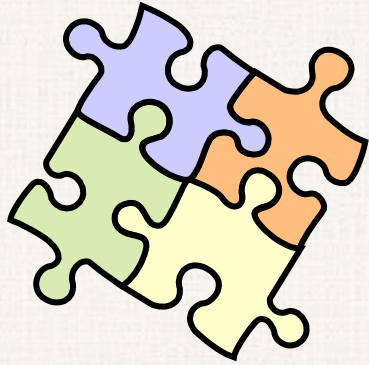
Thanks

Questions

?

Contact: *dmitra@cs.fit.edu*